Exhibit 23

Declaration of Dr. Renee McVay and Hillary Hull (July 3, 2020)

Plaintiffs' Motion For Summary Judgment

STATE OF NEW YORK, *et al.*, and ENVIRONMENTAL DEFENSE FUND
v.
ANDREW WHEELER, *et al.*
Civil Action No. 18-cv-0773 (RBW)

UNITED STATES DISTRICT COURT
FOR THE DISTRICT OF COLUMBIA

STATE OF NEW YORK, *et al.*, Plaintiffs, ENVIRONMENTAL DEFENSE FUND, Plaintiff-Intervenor, v. ANDREW WHEELER, *et al.*, Defendants.	Civil Action No. 18-cv-0773 (RBW)

DECLARATION OF DR. RENEE McVAY AND HILLARY HULL

We, Dr. Renee McVay and Hillary Hull, declare as follows:

1. I, Dr. Renee McVay, am a Senior Research Analyst in the Energy program at the Environmental Defense Fund ("EDF"). I earned my PhD in Chemical Engineering from the California Institute of Technology, where my research focused on atmospheric chemistry and the formation of atmospheric aerosols. I also have an MS in Chemical Engineering from the California Institute of Technology and a BS in Chemical Engineering from Texas A&M University. After my PhD, I completed a postdoctoral fellowship at the National Oceanic and Atmospheric Administration working with the regional air quality model WRF-Chem to improve performance and predictions of the model. At EDF, my work focuses on using emission inventories to develop state and region-specific emission profiles from the oil and gas sector. My curriculum vitae is attached as Attachment 1.

2. I, Hillary Hull, am a Senior Research and Analytics Manager for the Energy program at EDF. I have an MS from Stanford University in environmental engineering (Atmosphere & Energy Program) and a BS from the University of Texas at Austin in civil engineering. In my role at EDF, I develop analytics in support of EDF's state, federal, and international natural gas work. My work includes emissions inventory compilation, data and economic analytics, technical support for rulemaking and regulation, and policy analysis and development.

3. The Environmental Protection Agency ("EPA") has promulgated standards to reduce methane emissions at new and modified facilities in the oil and gas sector, *Oil and Natural Gas Sector Emission Standards for New, Reconstructed and Modified Sources*, 81 Fed. Reg. 35,824 (June 3, 2016) ("New Source Rule"). The standards reduce methane emissions by requiring regular leak detection and repair ("LDAR") and equipment upgrades at covered facilities in oil and natural gas production, processing, and transmission and storage segments. The New Source Rule has been fully in effect and securing reductions in methane at new and modified facilities for over four years.

4. We are aware that the New Source Rule triggers a legal obligation under Section 111(d) of the Clean Air Act, 42 U.S.C. § 7411(d), for EPA to issue emissions guidelines for existing sources ("Methane Guidelines"), but that EPA has not yet issued such guidelines.

5. We understand that EPA might finalize a proposed rule to revise the New Source Rule by removing methane as a regulated pollutant. EPA's proposal to remove methane regulation claims that, if finalized, the action will remove EPA's legal duty to adopt standards for existing oil and gas sources, but does not contain a quantitative assessment of the methane

pollution emitted by these sources or the foregone benefits of establishing existing source standards, as EPA is now required to do.

6. We performed an analysis to characterize sources that would be affected by Methane Guidelines, along with emissions from these sources, in order to document harm to the public from a continued delay by EPA in promulgating Methane Guidelines. Section I describes our methodology for identifying all affected sources and presents a map of affected wells. Section II characterizes total emissions that have occurred at affected facilities since the New Source Rule was promulgated in 2016, and quantifies the emissions that will result over the course of additional delay in adopting Methane Guidelines. Section III focuses on the local impacts of EPA's delay in issuing Methane Guidelines.

SECTION I: EPA's Continued Delay in Adopting Methane Guidelines Allows Hundreds of Thousands of Oil and Natural Gas Facilities to Forego Emissions Reductions.

7. To identify wells that would be subject to EPA Methane Guidelines, we obtained well data from Enverus (formerly known as DrillingInfo), a proprietary database that compiles a wide range of drilling- and production-related information from state oil and gas commissions. In September 2019, we obtained data for all wells in the U.S., filtering to include only onshore wells with active production during 2018 and 2019 in order to exclude abandoned and shuttered wells. We then excluded from the dataset wells that would be regulated as new or modified facilities under the New Source Rule.[1] The remaining wells, drilled or last modified before

[1] The New Source Rule applies to facilities "constructed, modified or reconstructed" after September 18, 2015—the date of EPA's proposed rule. 81 Fed. Reg. 35824, 35844 (June 3, 2016). As described above, *id.* at 35826, EPA's LDAR standards apply to new well sites and compressor stations that commenced construction after September 18, 2015. The standards also apply to modified well sites and compressor stations. The New Source Rule defines particular circumstances that constitute a modification at each of these facilities. For well sites, these include when a well at an existing site is fractured or re-fractured, an operation that is designed

September 18, 2015 (denoted as "existing wells"), would be covered by Methane Guidelines issued by EPA. In total, there are 855,271 producing existing wells that would be covered by EPA Methane Guidelines. Figure 1 displays a map of existing wells.

Figure 1: Map of Total Affected Well Sources

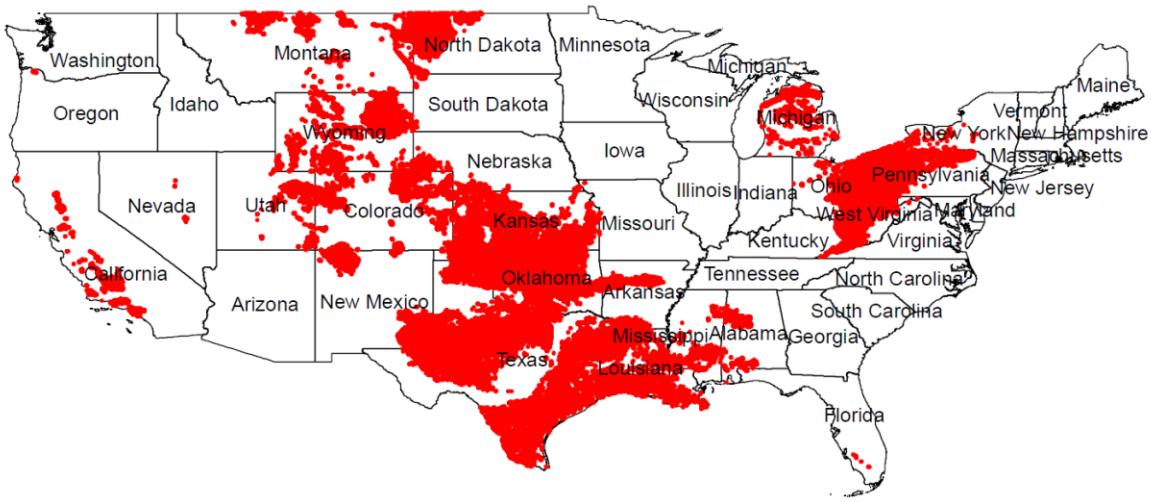

SECTION II: Delay by EPA in Adopting Methane Guidelines Has Resulted, and Will Continue to Result, in Substantial Emissions of Harmful Methane, Volatile Organic Compounds, and Hazardous Air Pollutants from Affected Facilities.

8. EPA's delay in promulgating Methane Guidelines for existing sources in the oil and natural gas sector has allowed substantial emissions of methane, VOC, and hazardous air pollutant ("HAP") emissions that would otherwise be remediated by Methane Guidelines.

---

to increase production of natural gas. 40 CFR § 60.5365a(i)(3). For compressor stations, the New Source Rule defines modifications to include the addition of a compressor at an existing station. 40 CFR § 60.5365a(j).

Enverus includes information on the "spud date" for wells, or the date on which drilling commenced. The database also includes information on well "completion dates," or the most recent date on which a well was cleared of flowback gas associated with hydraulic fracturing or re-fracturing. Using the database, we excluded wells with a spud date after September 18, 2015, which would be "new" for purposes of the 2016 Rule's LDAR requirements. Separately, we excluded wells with a spud date on or before September 18, 2015 but a completion date after September 18, 2015. This distinct category of sources includes both older, re-fractured wells and new wells with their initial fracture delayed to after September 18, 2015, which would be "modified" for purposes of the 2016 Rule's LDAR requirements.

Substantial emissions will continue as long as EPA continues to delay the promulgation of the Guidelines. Methane is a powerful short-term climate forcer with over 80 times the global warming potential of carbon dioxide on a mass basis over the first 20 years after it is emitted. VOCs react with nitrogen oxides to form ground-level ozone, or smog, which can cause respiratory disease and premature death. Other hazardous air pollutants emitted by oil and gas sources include benzene, a known human carcinogen.

9. We estimate the total emissions that have occurred at affected existing sources, as well as the amount of emissions that could have been prevented had EPA timely adopted Methane Guidelines. We further estimate the total amount of emissions that will continue to occur at affected existing sources in the near future if EPA continues to delay the promulgation of Methane Guidelines, as well as the amount of these emissions that could be prevented if Guidelines are adopted.

10. For this analysis, we assume that Methane Guidelines will extend the methane emissions reduction requirements found in the New Source Rule to all affected existing sources, specifically covering high-bleed pneumatic controllers at well sites and transmission and storage compressor stations, all continuous bleed pneumatic controllers at natural gas processing plants, equipment leaks from gas processing plants, well sites, and compressor stations, reciprocating and centrifugal compressors at both processing plants and compressor stations, and pneumatic pumps at well sites and processing plants. Though new technologies and best practices have shown promise of even greater emission reductions, we conservatively assume that the same technologies used in the New Source Rule would apply equally to existing sources. Several states that regulate both new and existing sources (including Colorado and California) largely apply the same measures at both sets of facilities, lending further support to this assumption.

11. To estimate the total emissions that have occurred at affected existing sources, as well as the amount of emissions that could be prevented had EPA adopted Methane Guidelines when it promulgated the New Source Rule, we used our EDF Methane Policy Analyzer model. Briefly, a baseline emissions inventory was developed for 2015, using a combination of EPA Greenhouse Gas Reporting Program data and previously published measurement studies, as reported in Alvarez et al 2018[2] for the alternative inventory (section S1.4). All emissions in 2015 were considered to be "existing" because the relevant date for the NSPS was near the end of 2015. We assumed that emissions attributable to existing sources decline year-over-year as existing sources are removed from operation or undertake modifications that subject them to regulation as modified sources under the New Source Rule based on a turnover rate of 5% for production sources, 4% for gathering and boosting sources, and 1% for all downstream sources. Emissions from sources subject to state regulations applicable to existing sources (California, Colorado, Utah, Wyoming in the Upper Green River Basin ozone non-attainment area, and Texas to a very limited extent) are subtracted from the projected emissions. We estimate that in the over four years since EPA has promulgated the New Source Rule, 38.5 million metric tons of methane have been emitted by existing oil and natural gas sources. We further estimate that 14.1 million metric tons of those methane emissions, or 37%, could have been avoided if Methane Guidelines were in effect and being implemented.

12. To estimate the total emissions that will continue to occur at affected existing sources if EPA continues to delay the promulgation of Methane Guidelines, as well as the amount of emissions that could be prevented if EPA promulgates Methane Guidelines, we extended the Methane Policy Analyzer to 2030. Each year that EPA delays promulgating

[2] Alvarez et al., *Assessment of Methane Emissions from the U.S. Oil and Gas Supply Chain*, 361 SCIENCE, 186–188 (2018), a true and accurate copy of which is attached as Exhibit 1.

Methane Guidelines will allow substantial additional emissions. For example, in 2021, 9.8 million metric tons of methane will be emitted by affected existing sources. We further estimate that 3.6 million metric tons of those methane emissions, or 37%, could be avoided if Methane Guidelines were in effect and being implemented. Table 1 summarizes the emissions allowed by EPA's delay in adopting Methane Guidelines, as well as the emissions reductions possible if Methane Guidelines were promulgated.

Table 1: Estimated Emissions at Affected Existing Sources and Potential Reductions Under Methane Guidelines

Time Period	Total Emissions from Affected Sources [metric tons]			Emissions that Could be Prevented by Methane Guidelines [metric tons]		
	Methane	VOC	HAPs	Methane	VOC	HAPs
2017	11,689,715	2,741,847	103,115	4,253,249	1,022,588	38,484
2018	11,099,151	2,597,590	97,684	4,067,664	977,969	36,805
2019	10,622,933	2,472,822	92,978	3,915,227	938,202	35,305
Total Emissions Since EPA Issued New Source Rule	**33,411,799**	**7,812,259**	**293,777**	**12,236,140**	**2,938,759**	**110,594**
2020	10,184,924	2,360,138	88,729	3,740,813	893,495	33,620
2021	9,785,180	2,256,193	84,809	3,583,294	852,460	32,072
2022	9,413,009	2,158,703	81,132	3,438,607	814,377	30,635
2023	9,025,023	2,059,736	77,402	3,287,058	775,799	29,181
2024	8,647,856	1,964,209	73,802	3,136,680	737,802	27,749
2025	8,294,707	1,874,858	70,434	2,997,488	702,609	26,423
2026	7,967,127	1,791,676	67,299	2,867,333	669,482	25,175
2027	7,657,181	1,712,896	64,330	2,744,475	638,148	23,994
2028	7,366,050	1,639,260	61,555	2,629,755	609,015	22,896
2029	7,099,500	1,571,426	58,998	2,524,569	582,076	21,880
2030	6,854,814	1,508,791	56,637	2,428,541	557,245	20,944

13. These emissions estimates, along with potential reductions, are conservative, as emerging data not reflected in the Methane Policy Analyzer indicates methane emissions from oil and gas sources in the United States are even greater than estimated in the Alvarez et al 2018 study. For example, Zhang et al 2020[3] documents significant oil and gas methane emissions at the basin level in the Permian Basin in Texas and New Mexico. Based on 11 months of satellite data encompassing 200,000 individual readings taken across the 160,000 square-kilometer basin by the European Space Agency's TROPOMI instrument from May 2018 to March 2019, the study found that Permian oil and gas operations are losing methane at a rate equal to 3.7% of their gas production. The peer-reviewed study estimated that annual methane emissions from oil and gas sources in the Permian basin are 2.7 million metric tons per year, more than twice as much as estimated for the region based on EPA's greenhouse gas inventory.

14. In its proposal to remove methane regulation, EPA claims that many states already regulate oil and gas methane emissions, and so a federal rule would be duplicative. 84 Fed. Reg. at 50,277. However, EPA has not analyzed in any meaningful way whether or not these state rules are applicable to existing sources. *Id.* at n. 104. We assessed the applicability of state standards to existing sources in California, Colorado, Montana, New Mexico, North Dakota, Ohio, Pennsylvania, Texas, Utah, and Wyoming (states that EPA includes in their "Comparison of State Oil and Natural Gas Regulations" table in their proposal to remove methane). These states take widely divergent approaches that vary significantly in stringency, and most states have no standards applicable to existing sources. Appendix 1 provides a detailed analysis of what state standards apply to existing sources.

[3] Zhang et al, *Quantifying methane emissions from the largest oil-producing basin in the United States from space*, Science Advances (April 22, 2020), *available at* https://advances.sciencemag.org/content/6/17/eaaz5120, a true and accurate copy of which is attached as Exhibit 2.

15. Our Methane Policy Analyzer allows us to also look at the projected reductions from state standards for existing sources. In 2020, state standards applicable to existing sources (certain standards in California, Colorado, Utah, Wyoming in the Upper Green River Basin ozone non-attainment area, and Texas) will reduce only 180,000 metric tons methane, roughly 5% of what federal Methane Guidelines could achieve.

SECTION III: EPA's Delay in Promulgating Methane Guidelines Has Resulted in, and Will Continue to Result in, Substantial Local Air Pollution

16. To look at the effect of EPA's delay on other harmful air pollution (including ozone-forming volatile organic compounds and hazardous air pollutants like benzene), we focus exclusively on production emissions because the Enverus database allows us to identify precisely where wells are located (and therefore emissions will occur). Because of that, we can assess emissions impacts in areas that already suffer from harmful levels of ambient air pollution, like ozone. As a result, the analysis in this section is not intended to capture the total, harmful emissions impact of the delay in adopting Methane Guidelines.

17. We have identified 97,000 wells that would be subject to Methane Guidelines in areas that are currently not in attainment with the 2015 national ambient air quality standards (NAAQS) for ozone. Appendix 2 provides a full list of nonattainment area counties with existing wells. These sources will add an estimated 160,000 metric tons of VOCs to the atmosphere annually if EPA continues to delay the adoption of Methane Guidelines. VOCs contribute to ozone formation and exacerbate smog-related health issues.

18. This estimate is conservative and does not fully capture the effects of EPA's delay in promulgating Methane Guidelines. The analysis does not account for the many affected wells located just outside of ozone non-attainment areas, which can still contribute to the formation of

ozone that can be transported into the non-attainment areas. Furthermore, the analysis in this section does not include additional emissions in these areas attributable to midstream and downstream segments that would be mitigated by Methane Guidelines.

19. By identifying existing well sites, we are also able to identify the local communities that are disproportionately impacted by the air pollution allowed by EPA's delay in promulgating Methane Guidelines. Using the US Census Bureau's American Community Survey 5-year estimates for 2012-2016, we were able to estimate the populations living within a half mile radius of the previously identified existing wells using areal apportionment. This method determines the area encompassed within a half mile buffer radius of all affected wells, and overlays those buffers onto census tracts to calculate the percentage of each tract comprised of buffers (i.e. the area of each tract within a half mile of an affected well). The areal apportionment method assumes that populations are spread evenly across a given census tract (excluding water bodies), and thus we are able to estimate the populations at a census tract level of those living within a half mile of an existing well. This method is commonly used in published literature utilizing distance-based analysis.[4] While some studies have used finer spatial resolutions such as census block groups, we performed our analysis using census tracts in order to minimize margin of error in census estimates. Census tracts, and even larger regions such as zip codes, have often been used in similar analyses.[5] We used a half mile radius because recent scientific evidence

[4] *See, e.g.* J. C. S. Long, L. Feinstein, J. T. Birkholzer, W. Foxall, "An Independent Scientific Assessment Of Well Stimulation In California, Vol. 3" (California Council on Science and Technology, 2016), *available at* https://ccst.us/publications/2015/2015SB4-v3.php; J. Chakraborty, J. A. Maantay, J. D. Brender, Disproportionate Proximity to Environmental Health Hazards: Methods, Models, and Measurement. American Journal of Public Health. 101, S27–S36 (2011).

[5] *See, e.g.*, T. Srebotnjak and M. Rotkin-Ellman, "Drilling in California: Who's at risk?" Natural Resources Defense Council, 2014; Mohai P, Saha R. Reassessing racial and socio-economic disparities in environmental justice research. Demography. 2006;43(2):383–399; Kearney G, Kiros GE. A spatial evaluation of socio demographics surrounding National Priorities List sites in Florida using a distance-based approach. Int J Health Geogr. 2009;8:33.

indicates close proximity to oil and gas development is associated with HAP exposure and other adverse health impacts for local populations. *See* Declaration of Ananya Roy and Tammy Thompson.

20. Using this methodology, we find that approximately 9,300,000 people live within half a mile of an existing well in the U.S., including 600,000 children under the age of five years and 1,400,000 elderly people over the age of 65 years, who are especially sensitive to the health risks posed by ozone and other local air pollution. Additionally, approximately 1,400,000 people living below the poverty line, who may face greater barriers such as accessing medical care, and nearly 2,800,000 people of color live within half a mile of an existing well.

Conclusion

21. EPA's delay in adopting Methane Guidelines for existing sources has already allowed significant air pollution. If this litigation is stayed, any continued delay in promulgating Methane Guidelines requirements will allow numerous sources to continue operating without controls to reduce methane, VOC, and HAP emissions, allowing significant emissions to persist from these sources with each additional year of delay.

I declare under the penalty of perjury that the foregoing is true and correct.

Renee McVay

Renee McVay

July 3, 2020

I declare that the foregoing is true and correct.

/s/ Hillary Hull
Hillary Hull

July 3, 2020

Appendix 1

State Standards Applicable to Existing Source Emissions

In its proposal to remove methane regulation, EPA claims that many states already regulate oil and gas methane emissions, and so a federal rule would be duplicative. However, EPA has not analyzed in any meaningful way whether or not these state rules are applicable to existing sources. Many states' regulations are only applicable to new sources, and thus would not apply to any existing sources. Of the ten states EPA includes in their "Comparison of State Oil and Natural Gas Regulations" table, 84 Fed. Reg. 50,277—California (CA), Colorado (CO), Montana (MT), New Mexico (NM), North Dakota (ND), Ohio (OH), Pennsylvania (PA), Texas (TX), Utah (UT), and Wyoming (WY), only six states were proposed by EPA to be considered for equivalency to the 2016 NSPS OOOOa[6] (CA, CO, OH, and PA for well sites and compressor stations, TX & UT for well sites only). Only five states currently have oil and gas regulations that would apply to any existing sources: California, Colorado, Utah, Wyoming, and Texas. (Montana, New Mexico, and North Dakota have either very weak permits or guidance applicable to existing sources that EPA previously determined were not equivalent to the NSPS). In Wyoming, only existing sources within the Upper Green River Basin above a certain emissions threshold are covered, so the majority of existing sources within that state are not covered. Texas regulations have various effective dates depending on the location of a facility, but at least one regulation applies to new sources that were constructed/modified after September 2000. Because this date predates the NSPS effective date, some sources considered "existing" for the NSPS will be considered "new" under Texas regulations. However, as detailed below, Texas regulations

[6] EPA, Memorandum: Equivalency of State Fugitive Emissions Programs for Well Sites and Compressor Stations to Proposed Standards at 40 CFR Part 60, Subpart OOOOa (April 12, 2018), *available at* https://www.regulations.gov/document?D=EPA-HQ-OAR-2017-0483-0041.

apply to significantly fewer sources than the NSPS. More detail on each state's regulation is provided below:

California's oil and gas methane regulations, adopted by the California Air Resources Board in 2017, apply to both new and existing sources in the production, processing, and transmission and storage segments and took effect in 2018/2019. These requirements apply to pneumatic controllers, pumps, compressors, fugitive emission components, and storage tanks.

Colorado oil and gas regulations apply to both new and existing sources. The regulations cover equipment leaks at well sites and compressor stations (tiered LDAR frequency tied to VOC emissions), pneumatic controllers at well sites and processing plants, liquids unloading, tanks at well sites with VOC emissions greater than 6 tons per year (tpy), associated gas venting, oil well completions, centrifugal compressors at well sites and processing plants, reciprocating compressors at processing plants, and dehydrators at well sites and processing plants. Regulations were adopted in 2014 and initially took effect in 2015, with updates to strengthen leak detection and repair standards in 2017 and 2019. In 2019 the state also decreased the emission control threshold for storage tanks and added a new control requirement for new and existing storage tank unloading operations.

Montana's air quality permits cover oil and gas well facilities that were completed or modified after March 16, 1979 (beginning on July 1, 2006). While this is prior to the NSPS effective date, it does not cover all existing facilities. Additionally, facilities must have a potential to emit more than 25 tpy of VOC (or other specified pollutant not including methane), which will not cover all well sites covered by the NSPS. Monitoring only includes "VOC piping components" using AVO, a monitoring method considered inadequate by the EPA. Montana's regulation also does not cover compressor stations. If the EPA does not consider Montana

adequately equivalent to the NSPS for new and modified sources, it should not consider it adequate for existing sources either.

While the New Mexico Administrative Code restricts production operators from allowing gas to "leak or escape", it does not specify whether this restriction applies to new or existing facilities, or how it enforces this requirement. Even though, as shown in Table 9, it technically covers well sites and storage vessels, the EPA could not evaluate its equivalency to the NSPS in 2018 because they were unable to determine the enforcement mechanism. Current New Mexico regulations therefore should not be considered to contribute to any meaningful emissions reductions should the primary proposal be finalized. The New Mexico Environment Department and New Mexico Energy, Minerals and Natural Resources Department are each in the process of developing rules that will regulate methane emissions from new and existing oil and gas facilities.

North Dakota regulations cover new and modified wells as of July 1, 1970. North Dakota exempts low-production wells from all monitoring (<15 bbl/day) and does not monitor compressor stations. Additionally, North Dakota's regulation is enforced through company-wide consent decrees, which are negotiated terms for non-compliance and include an expiration data (after which the companies return to compliance). Due to the flexible and temporary nature of these consent decrees, the EPA determined in 2018 that North Dakota's regulation was not equivalent to the NSPS. Even if the compliance could be guaranteed, approximately 4% of the wells covered by the NSPS would be exempt from regulation in North Dakota in addition to all wells existing before 1970.

Pennsylvania's current LDAR program covers unconventional well sites and gathering and boosting compressor stations that are new and modified relative to August 8, 2018. In

December 2019, Pennsylvania issued a proposal to regulate VOC from existing well sites in the state.

Utah regulations apply to both new and existing sources. New sources were covered beginning in 2014, and existing sources were added in 2018. Regulations for well sites cover equipment leaks, tanks (with an emissions threshold), dehydrators, associated gas venting, and pneumatics. Regulations for processing plants and compressor stations cover pneumatics. Utah state regulations do not apply on tribal lands (approximately 20% of emissions are on tribal lands).

When analyzing the equivalency of Wyoming's regulation to the 2016 NSPS OOOOa, the EPA considered the version of Wyoming DEQ's regulation of PAD facilities that was finalized prior to that analysis in 2018. Since that analysis was conducted, Wyoming has released a more comprehensive update to that rule. While this update expands coverage to well sites outside of the Upper Green River Basin, many of the issues which prevented EPA from considering the previous rule adequate still apply. Wyoming regulations apply to new sources, as well as existing sources within the Upper Green River Basin (UGRB) (a nonattainment area). Regulations cover equipment leaks, pneumatic controllers, tanks (with an emissions threshold), oil well completions, pneumatic pumps, and dehydrators (with an emissions threshold). Less than 20% of total production emissions are within the UGRB. While the monitoring frequency and monitoring instrument are acceptable, there is no specified initial monitoring date or repair deadline for facilities with emissions greater than or equal to 4 TPY of VOCs within the UGRB.

Texas regulations apply to new sources, relative to either 2000, 2011, or 2012 depending on location and type of permit. Texas requires a leak detection and repair ("LDAR") program for certain mid-sized to large oil and gas facilities. The specific requirements vary depending on the

facility's location and potential to emit uncontrolled volatile organic compounds ("VOC"). Most well sites are not subject to LDAR due to the high emissions threshold uncontrolled VOC emissions (>10 or 25 tpy) and distance from a sensitive receptor, such as a home or school, that triggers the application of LDAR. EDF analysis of Texas Standard Permits found that only roughly 5.5% of well sites in Texas are required to conduct LDAR.

Appendix 2

Counties with wells that would be subject to Methane Guidelines in areas that are currently not in attainment with the 2015 national ambient air quality standards (NAAQS) for ozone are as follows:

Chambers (TX), Brazoria (TX), Harris (TX), Montgomery (TX), Galveston (TX), Fort Bend (TX), Parker (TX), Hood (TX), Palo Pinto (TX), Wise (TX), Jack (TX), Denton (TX), Tarrant (TX), Bexar (TX), Johnson (TX), Duchesne (UT), Uintah (UT), Los Angeles (CA), Orange (CA), San Bernardino (CA), Ventura (CA), San Luis Obispo (CA), Kern (CA), Tulare (CA), Fresno (CA), Kings (CA), Alameda (CA), Sacramento (CA), San Joaquin (CA), Solano (CA), Yolo (CA), Madera (CA), Santa Clara (CA), Contra Costa (CA), Adams (CO), Arapahoe (CO), Boulder (CO), Denver (CO), Larimer (CO), Weld (CO), Broomfield (CO), Ellis (TX), St Clair (MI), Oakland (MI), Livingston (MI), Macomb (MI), Wayne (MI), Washtenaw (MI), Allegan (MI), Monroe (MI), Muskegon (MI), Cuyahoga (OH), Delaware (OH), Fairfield (OH), Geauga (OH), Lake (OH), Licking (OH), Lorain (OH), Medina (OH), Portage (OH), Summit (OH), Mahoning (OH), Hill (TX), Dallas (TX), Kaufman (TX), Atascosa (TX), Morgan (CO)

Attachment 1

Renee C. McVay

Environmental Defense Fund
301 Congress Ave, Suite 1300, Austin, TX 78701
Email: rmcvay@edf.org, Phone: (512) 691-3474

Education

Ph.D., Chemical Engineering ***2016***
California Institute of Technology Pasadena, CA
Advisor: Dr. John H. Seinfeld
National Science Foundation Graduate Research Fellowship (GRFP)
National Science Foundation Graduate Research Opportunities Worldwide (GROW) Award

M.S., Chemical Engineering ***2014***
California Institute of Technology Pasadena, CA
Advisor: Dr. John H. Seinfeld GPA: 4.0

B.S., Chemical Engineering ***2011***
Texas A&M University College Station, TX
Minors in Chemistry and Spanish GPA: 4.0
International Engineering Certificate

Experience

Environmental Defense Fund Austin, TX
Senior Research Analyst 2017-Present
Research Focus: Using emission inventories to develop state and region-specific emission profiles from the oil and gas sector.

Cooperative Institute for Research in Environmental Sciences (CIRES) Boulder, CO
Postdoctoral Fellow 2016-2017
Research Focus: Modeling atmospheric chemistry and secondary organic aerosol (SOA) formation using the Weather Research and Forecasting model coupled to Chemistry (WRF-Chem).

California Institute of Technology Pasadena, CA
Ph.D. Candidate 2011-2016
Advisor: Dr. John H. Seinfeld
Research Focus: Modeling secondary organic aerosol (SOA) formation from the gas-phase oxidation of volatile organic compounds to compare with experimental observations in environmental chambers

Laboratoire Interuniversitaire des Systèmes Atmosphériques Paris, France
International Research Collaboration Jan-May 2015
Advisor: Dr. Bernard Aumont
Research Focus: Working with and updating the Generator for Explicit Chemistry and Kinetics of Organics in the Atmosphere (GECKO-A) and comparing model predictions to experimental observations

Eastman Chemical Company Longview, TX
Engineering Intern Summer 2010
Job Focus: Material balances, rate studies, and sampling programs

Publications and Presentations

Peer-Reviewed Journal Publications
Schwantes, Rebecca H., Katherine A. Schilling, Renee C. McVay, Hanna Lignell, Matthew M. Coggon, Xuan Zhang, Paul O. Wennberg, and John H. Seinfeld. Formation of Highly Oxygenated Low-Volatility Products from Cresol Oxidation, *Atmos. Chem. Phys. Discuss.*, **2017**, *17*, 3453-3474, doi:10.5194/acp-17-3453-201.

T. Nah, R. C. McVay, J. R. Pierce, J. H. Seinfeld, and N. L. Ng. Constraining uncertainties in particle wall-deposition correction during SOA formation in chamber experiments, *Atmos. Chem. Phys.*, **2017**, *17*, 2297-2310 doi:10.5194/acp-17-2297-2017.

Nah, Theodora, Renee C. McVay, Xuan Zhang, Christopher M. Boyd, John H. Seinfeld, and Nga L. Ng. Influence of Seed Aerosol Surface Area and Oxidation Rate on Vapor-Wall Deposition and SOA Mass Yields: A case study with α-pinene Ozonolysis, *Atmos. Chem. Phys.*, **2016**, *16*, 9361-9379, doi:10.5194/acp-16-9361-2016.

McVay, Renee C., Xuan Zhang, Bernard Aumont, Richard Valorso, Marie Camredon, Yuyi S. La, Paul Wennberg and John H. Seinfeld. SOA formation from the photooxidation of α-pinene: Systematic exploration of the simulation of chamber data, *Atmos. Chem. Phys.*, **2016**, *16*, 2785-2802, doi:10.5194/acp-16-2785-2016.

Zhang, Xuan, Renee C. McVay, Dan D. Huang, Nathan F. Dalleska, Bernard Aumont, Richard E. Flagan, and John H. Seinfeld. Formation and evolution of molecular products in α-pinene secondary organic aerosol. *Proc. Natl. Acad. Sci.*, **2015**, *112*, 14168-14173, doi:10.1073/pnas.1517742112.

Zhang, X., R. H. Schwantes, R. C. McVay, H. Lignell, M. M. Coggon, R. C. Flagan, and J. H. Seinfeld. Vapor wall deposition in Teflon chambers. *Atmos. Chem. Phys.*, **2015,** *15*, 4197-4214.

McVay, Renee, Christopher Cappa, and John Seinfeld. Vapor Wall Deposition in Chambers: Theoretical Considerations. *Environ. Sci. and Technol.*, **2014**, *48*, 10251-10258.

Zhang, Xuan, Christopher Cappa, Shantanu Jathar, Renee McVay, Joseph Ensberg, Michael Kleeman, and John Seinfeld. Influence of vapor wall loss in laboratory chambers on yields of secondary organic aerosol. *Proc. Natl. Acad. Sci.*, **2014**, *111*, 5802-5807.

Conference Presentations

McVay, Renee, Theodora Nah, Jeffrey R. Pierce, John Seinfeld, Nga Lee Ng. Uncertainties in Particle Wall Loss Correction during Secondary Organic Aerosol Formation in Chamber Experiments. American Association for Aerosol Research, 27-21 October 2016, Portland.

McVay, Renee, Xuan Zhang, Bernard Aumont, Richard Valorso, Marie Camredon, Stéphanie La, and John Seinfeld. Uncertainties in SOA Formation from the Photooxidation of α-pinene. American Geophysical Union, 14-18 December 2015, San Francisco.

McVay, Renee, Xuan Zhang, Christopher Cappa, and John Seinfeld. Vapor Wall Loss in Chambers: Theoretical Considerations. American Geophysical Union, 15-19 December 2014, San Francisco.

GREENHOUSE GASES

Assessment of methane emissions from the U.S. oil and gas supply chain

Ramón A. Alvarez[1]*, Daniel Zavala-Araiza[1], David R. Lyon[1], David T. Allen[2], Zachary R. Barkley[3], Adam R. Brandt[4], Kenneth J. Davis[3], Scott C. Herndon[5], Daniel J. Jacob[6], Anna Karion[7], Eric A. Kort[8], Brian K. Lamb[9], Thomas Lauvaux[3], Joannes D. Maasakkers[6], Anthony J. Marchese[10], Mark Omara[1], Stephen W. Pacala[11], Jeff Peischl[12,13], Allen L. Robinson[14], Paul B. Shepson[15], Colm Sweeney[13], Amy Townsend-Small[16], Steven C. Wofsy[6], Steven P. Hamburg[1]

Methane emissions from the U.S. oil and natural gas supply chain were estimated by using ground-based, facility-scale measurements and validated with aircraft observations in areas accounting for ~30% of U.S. gas production. When scaled up nationally, our facility-based estimate of 2015 supply chain emissions is 13 ± 2 teragrams per year, equivalent to 2.3% of gross U.S. gas production. This value is ~60% higher than the U.S. Environmental Protection Agency inventory estimate, likely because existing inventory methods miss emissions released during abnormal operating conditions. Methane emissions of this magnitude, per unit of natural gas consumed, produce radiative forcing over a 20-year time horizon comparable to the CO_2 from natural gas combustion. Substantial emission reductions are feasible through rapid detection of the root causes of high emissions and deployment of less failure-prone systems.

Methane (CH_4) is a potent greenhouse gas, and CH_4 emissions from human activities since preindustrial times are responsible for 0.97 W m^{-2} of radiative forcing, as compared to 1.7 W m^{-2} for carbon dioxide (CO_2) (*1*). CH_4 is removed from the atmosphere much more rapidly than CO_2; thus, reducing CH_4 emissions can effectively reduce the near-term rate of warming (*2*). Sharp growth in U.S. oil and natural gas (O/NG) production beginning around 2005 (*3*) raised concerns about the climate impacts of increased natural gas use (*4*, *5*). By 2012, disagreement among published estimates of CH_4 emissions from U.S. natural gas operations led to a broad consensus that additional data were needed to better characterize emission rates (*4*–*7*). A large body of field measurements made between 2012 and 2016 (table S1) has markedly improved understanding of the sources and magnitude of CH_4 emissions from the industry's operations. Brandt *et al.* summarized the early literature (*8*); other assessments incorporated elements of recent data (*9*–*11*). This work synthesizes recent studies to provide an improved overall assessment of emissions from the O/NG supply chain, which we define to include all operations associated with O/NG production, processing, and transport (materials and methods, section S1.0) (*12*).

Measurements of O/NG CH_4 emissions can be classified as either top-down (TD) or bottom-up (BU). TD studies quantify ambient methane enhancements using aircraft, satellites, or tower networks and infer aggregate emissions from all contributing sources across large geographies. TD estimates for nine O/NG production areas have been reported to date (table S2). These areas are distributed across the U.S. (fig. S1) and account for ~33% of natural gas, ~24% of oil production, and ~14% of all wells (*13*). Areas sampled in TD studies also span the range of hydrocarbon characteristics (predominantly gas, predominantly oil, or mixed), as well as a range of production characteristics such as well productivity and maturity. In contrast, BU studies generate regional, state, or national emission estimates by aggregating and extrapolating measured emissions from individual pieces of equipment, operations, or facilities, using measurements made directly at the emission point or, in the case of facilities, directly downwind.

Recent BU studies have been performed on equipment or facilities that are expected to represent the vast majority of emissions from the O/NG supply chain (table S1). In this work, we integrate the results of recent facility-scale BU studies to estimate CH_4 emissions from the U.S. O/NG supply chain, and then we validate the results using TD studies (materials and methods). The probability distributions of our BU methodology are based on observed facility-level emissions, in contrast to the component-by-component approach used for conventional inventories. We thus capture enhancements produced by all sources within a facility, including the heavy tail of the distribution. When the BU estimate is developed in this manner, direct comparison of BU and TD estimates of CH_4 emissions in the nine basins for which TD measurements have been reported indicates agreement between methods, within estimated uncertainty ranges (Fig. 1).

Our national BU estimate of total CH_4 emissions in 2015 from the U.S. O/NG supply chain is 13 (+2.1/−1.6, 95% confidence interval) Tg CH_4/year (Table 1). This estimate of O/NG CH_4 emissions can also be expressed as a production-normalized emission rate of 2.3% (+0.4%/−0.3%) by normalizing by annual gross natural gas production [33 trillion cubic feet (*13*), with average CH_4 content of 90 volume %]. Roughly 85% of national BU emissions are from production, gathering, and processing sources, which are concentrated in active O/NG production areas.

Our assessment does not update emissions from local distribution and end use of natural gas, owing to insufficient information addressing this portion of the supply chain. However, recent studies suggest that local distribution emissions exceed the current inventory estimate (*14*–*16*), and that end-user emissions might also be important. If these findings prove to be representative, overall emissions from the natural gas supply chain would increase relative to the value in Table 1 (materials and methods, section S1.5).

Our BU method and TD measurements yield similar estimates of U.S. O/NG CH_4 emissions in 2015, and both are significantly higher than the corresponding estimate in the U.S. Environmental Protection Agency's Greenhouse Gas Inventory (EPA GHGI) (Table 1 and materials and methods, section S1.3) (*17*). Discrepancies between TD estimates and the EPA GHGI have been reported previously (*8*, *18*). Our BU estimate is 63% higher than the EPA GHGI, largely due to a more than twofold difference in the production segment (Table 1). The discrepancy in production sector emissions alone is ~4 Tg CH_4/year, an amount larger than the emissions from any other O/NG supply chain segment. Such a large difference cannot be attributed to expected uncertainty in either estimate: The extremal ends of the 95% confidence intervals for each estimate differ by 20% (i.e., ~12 Tg/year for the lower bound of our BU estimate can be compared to ~10 Tg/year for the upper bound of the EPA GHGI estimate).

We believe the reason for such large divergence is that sampling methods underlying conventional inventories systematically underestimate total emissions because they miss high emissions caused by abnormal operating conditions (e.g., malfunctions). Distributions of measured emissions from production sites in BU studies are invariably "tail-heavy," with large emission rates measured at a small subset of sites at any single point in time (*19*–*22*). Consequently, the most likely hypothesis for the difference between the EPA GHGI and BU estimates derived from facility-level measurements is that measurements used to develop GHGI emission factors

[1]Environmental Defense Fund, Austin, TX, USA. [2]University of Texas at Austin, Austin, TX, USA. [3]The Pennsylvania State University, University Park, PA, USA. [4]Stanford University, Stanford, CA, USA. [5]Aerodyne Research Inc., Billerica, MA, USA. [6]Harvard University, Cambridge, MA, USA. [7]National Institute of Standards and Technology, Gaithersburg, MD, USA. [8]University of Michigan, Ann Arbor, MI, USA. [9]Washington State University, Pullman, WA, USA. [10]Colorado State University, Fort Collins, CO, USA. [11]Princeton University, Princeton, NJ, USA. [12]University of Colorado, CIRES, Boulder, CO, USA. [13]NOAA Earth System Research Laboratory, Boulder, CO, USA. [14]Carnegie Mellon University, Pittsburgh, PA, USA. [15]Purdue University, West Lafayette, IN, USA. [16]University of Cincinnati, Cincinnati, OH, USA.
*Corresponding author. Email: ralvarez@edf.org

undersample abnormal operating conditions encountered during the BU work. Component-based inventory estimates like the GHGI have been shown to underestimate facility-level emissions (*23*), probably because of the technical difficulty and safety and liability risks associated with measuring large emissions from, for example, venting tanks such as those observed in aerial surveys (*24*).

Abnormal conditions causing high CH_4 emissions have been observed in studies across the O/NG supply chain. An analysis of site-scale emission measurements in the Barnett Shale concluded that equipment behaving as designed could not explain the number of high-emitting production sites in the region (*23*). An extensive aerial infrared camera survey of ~8000 production sites in seven U.S. O/NG basins found that ~4% of surveyed sites had one or more observable high–emission rate plumes (*24*) (detection threshold of ~3 to 10 kg CH_4/hour was two to seven times higher than mean production site emissions estimated in this work). Emissions released from liquid storage tank hatches and vents represented 90% of these sightings. It appears that abnormal operating conditions must be largely responsible, because the observation frequency was too high to be attributed to routine operations like condensate flashing or liquid unloadings alone (*24*). All other observations were due to anomalous venting from dehydrators, separators, and flares. Notably, the two largest sources of aggregate emissions in the EPA GHGI—pneumatic controllers and equipment leaks—were never observed from these aerial surveys. Similarly, a national survey of gathering facilities found that emission rates were four times higher at the 20% of facilities where substantial tank venting emissions were observed, as compared to the 80% of facilities without such venting (*25*). In addition, very large emissions from leaking isolation valves at transmission and storage facilities were quantified by means of downwind measurement but could not be accurately (or safely) measured by on-site methods (*26*). There is an urgent need to complete equipment-based measurement campaigns that capture these large-emission events, so that their causes are better understood.

In contrast to abnormal operational conditions, alternative explanations such as outdated component emission factors are unlikely to explain the magnitude of the difference between our facility-based BU estimate and the GHGI. First, an equipment-level inventory analogous to the EPA GHGI but updated with recent direct measurements of component emissions (materials and methods, section S1.4) predicts total production emissions that are within ~10% of the EPA GHGI, although the contributions of individual source categories differ significantly (table S3). Second, we consider unlikely an alternative hypothesis that systematically higher emissions during daytime sampling cause a high bias in TD methods (materials and methods, section S1.6). Two other factors may lead to low bias in EPA GHGI and similar inventory estimates. Operator cooperation is required to obtain site access for emission measurements (*8*). Operators with lower-emitting sites are plausibly more likely to cooperate in such studies, and workers are likely to be more careful to avoid errors or fix problems when measurement teams are on site or about to arrive. The potential bias due to this "opt-in" study design is very challenging to determine. We therefore rely primarily on site-level, downwind measurement methods with limited or no operator forewarning to construct our BU estimate. Another possible source of bias is measurement error. It has been suggested that malfunction of a measurement instrument widely used in the O/NG industry contributes to underestimated emissions in inventories (*27*); however, this cannot explain the more than twofold difference in production emissions (*28*).

The tail-heavy distribution for many O/NG CH_4 emission sources has important implications for mitigation because it suggests that most sources—whether they represent whole facilities or individual pieces of equipment—can have lower emissions when they operate as designed. We anticipate that significant emissions reductions could be achieved by deploying well-designed emission detection and repair systems that are capable of identifying abnormally operating facilities or equipment. For example, pneumatic controllers and equipment leaks are the largest emission sources in the O/NG production segment exclusive of missing emission sources (38 and 21%, respectively; table S3), with malfunctioning controllers contributing 66% of total pneumatic controller emissions (materials and methods, section S1.4) and equipment leaks 60% higher than the GHGI estimate.

Table 1. Summary of this work's bottom-up estimates of CH_4 emissions from the U.S. oil and natural gas (O/NG) supply chain (95% confidence interval) and comparison to the EPA Greenhouse Gas Inventory (GHGI).

Industry segment	2015 CH_4 emissions (Tg/year)	
	This work (bottom-up)	EPA GHGI (*17*)
Production	7.6 (+1.9/−1.6)	3.5
Gathering	2.6 (+0.59/−0.18)	2.3
Processing	0.72 (+0.20/−0.071)	0.44
Transmission and storage	1.8 (+0.35/−0.22)	1.4
Local distribution*	0.44 (+0.51/−0.22)	0.44
Oil refining and transportation*	0.034 (+0.050/−0.008)	0.034
U.S. O/NG total	13 (+2.1/−1.7)	8.1 (+2.1/−1.4)†

*This work's emission estimates for these sources are taken directly from the GHGI. The local distribution estimate is expected to be a lower bound on actual emissions and does not include losses downstream of customer meters due to leaks or incomplete combustion (materials and methods, section S1.5).
†The GHGI only reports industry-wide uncertainties.

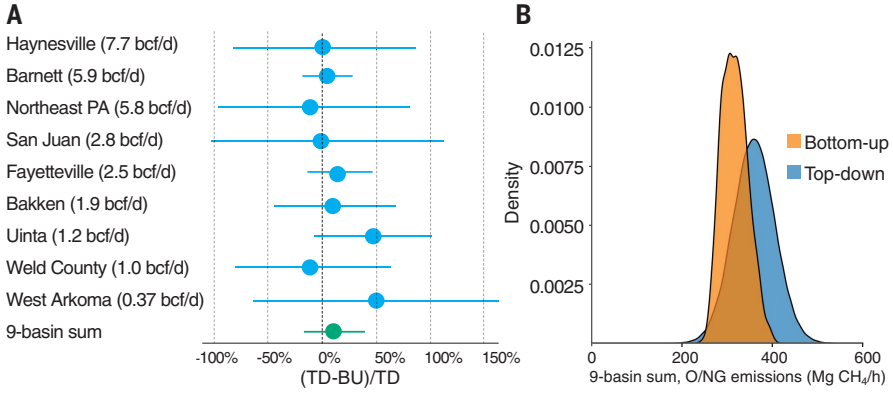

Fig. 1. Comparison of this work's bottom-up (BU) estimates of methane emissions from oil and natural gas (O/NG) sources to top-down (TD) estimates in nine U.S. O/NG production areas. (**A**) Relative differences of the TD and BU mean emissions, normalized by the TD value, rank ordered by natural gas production in billion cubic feet per day (bcf/d, where 1 bcf = 2.8×10^7 m^3). Error bars represent 95% confidence intervals. (**B**) Distributions of the nine-basin sum of TD and BU mean estimates (blue and orange probability density, respectively). Neither the ensemble of TD-BU pairs (A) nor the nine-basin sum of means (B) are statistically different [$p = 0.13$ by a randomization test, and mean difference of 11% (95% confidence interval of −17 to 41%)].

Gathering operations, which transport unprocessed natural gas from production sites to processing plants or transmission pipelines, produce ~20% of total O/NG supply chain CH_4 emissions. Until the publication of recent measurements (*29*), these emissions were largely unaccounted by the EPA GHGI. Gas processing, transmission and storage together contribute another ~20% of total O/NG supply chain emissions, most of which come from ~2500 processing and compression facilities.

Our estimate of emissions from the U.S. O/NG supply chain (13 Tg CH_4/year) compares to the EPA estimate of 18 Tg CH_4/year for all other anthropogenic CH_4 sources (*17*). Natural gas losses are a waste of a limited natural resource (~$2 billion/year), increase global levels of surface ozone pollution (*30*), and substantially erode the potential climate benefits of natural gas use. Indeed, our estimate of CH_4 emissions across the supply chain, per unit of gas consumed, results in roughly the same radiative forcing as does the CO_2 from combustion of natural gas over a 20-year time horizon (31% over 100 years). Moreover, the climate impact of 13 Tg CH_4/year over a 20-year time horizon roughly equals that from the annual CO_2 emissions from all U.S. coal-fired power plants operating in 2015 (31% of the impact over a 100-year time horizon) (materials and methods, section S1.7).

We suggest that inventory methods would be improved by including the substantial volume of missing O/NG CH_4 emissions evident from the large body of scientific work now available and synthesized here. Such empirical adjustments based on observed data have been previously used in air quality management (*31*).

The large spatial and temporal variability in CH_4 emissions for similar equipment and facilities (due to equipment malfunction and other abnormal operating conditions) reinforces the conclusion that substantial emission reductions are feasible. Key aspects of effective mitigation include pairing well-established technologies and best practices for routine emission sources with economically viable systems to rapidly detect the root causes of high emissions arising from abnormal conditions. The latter could involve combinations of current technologies such as on-site leak surveys by company personnel using optical gas imaging (*32*), deployment of passive sensors at individual facilities (*33*, *34*) or mounted on ground-based work trucks (*35*), and in situ remote-sensing approaches using tower networks, aircraft, or satellites (*36*). Over time, the development of less failure-prone systems would be expected through repeated observation of and further research into common causes of abnormal emissions, followed by re-engineered design of individual components and processes.

REFERENCES AND NOTES

1. G. Myhre *et al*., in *Climate Change 2013: The Physical Science Basis. Contribution of Working Group I to the Fifth Assessment Report of the Intergovernmental Panel on Climate Change* (Cambridge Univ. Press, Cambridge, UK, 2013); www.ipcc.ch/pdf/assessment-report/ar5/wg1/WG1AR5_Chapter08_FINAL.pdf.
2. J. K. Shoemaker, D. P. Schrag, M. J. Molina, V. Ramanathan, *Science* **342**, 1323–1324 (2013).
3. U.S. Energy Information Administration (EIA), "Annual Energy Outlook 2017" (EIA, 2017); www.eia.gov/outlooks/aeo/.
4. R. W. Howarth, R. Santoro, A. Ingraffea, *Clim. Change* **106**, 679–690 (2011).
5. R. A. Alvarez, S. W. Pacala, J. J. Winebrake, W. L. Chameides, S. P. Hamburg, *Proc. Natl. Acad. Sci. U.S.A.* **109**, 6435–6440 (2012).
6. U.S. Department of Energy (DOE), "Ninety-day report of the Secretary of Energy Advisory Board's Shale Gas Subcommittee" (2011); https://energy.gov/downloads/90-day-interim-report-shale-gas-production-secretary-energy-advisory-board.
7. National Petroleum Council (NPC), "Prudent Development: Realizing the Potential of North America's Abundant Natural Gas and Oil Resources" (NPC, 2011); www.npc.org.
8. A. R. Brandt *et al*., *Science* **343**, 733–735 (2014).
9. D. T. Allen, *J. Air Waste Manag. Assoc.* **66**, 549–575 (2016).
10. P. Balcombe, K. Anderson, J. Speirs, N. Brandon, A. Hawkes, *ACS Sustain. Chem.& Eng.* **5**, 3–20 (2017).
11. J. A. Littlefield, J. Marriott, G. A. Schivley, T. J. Skone, *J. Clean. Prod.* **148**, 118–126 (2017).
12. See supplementary materials.
13. Drillinginfo, Inc., Drillinginfo Production Query (2015); https://info.drillinginfo.com/.
14. K. McKain *et al*., *Proc. Natl. Acad. Sci. U.S.A.* **112**, 1941–1946 (2015).
15. B. K. Lamb *et al*., *Environ. Sci. Technol.* **50**, 8910–8917 (2016).
16. D. Wunch *et al*., *Atmos. Chem. Phys.* **16**, 14091–14105 (2016).
17. U.S. Environmental Protection Agency (EPA), "Inventory of U.S. Greenhouse Gas Emissions and Sinks: 1990-2015" (EPA, 2017); www.epa.gov/ghgemissions/inventory-us-greenhouse-gas-emissions-and-sinks-1990-2015.
18. D. Zavala-Araiza *et al*., *Proc. Natl. Acad. Sci. U.S.A.* **112**, 15597–15602 (2015).
19. C. W. Rella, T. R. Tsai, C. G. Botkin, E. R. Crosson, D. Steele, *Environ. Sci. Technol.* **49**, 4742–4748 (2015).
20. M. Omara *et al*., *Environ. Sci. Technol.* **50**, 2099–2107 (2016).
21. A. M. Robertson *et al*., *Environ. Sci. Technol.* **51**, 8832–8840 (2017).
22. A. R. Brandt, G. A. Heath, D. Cooley, *Environ. Sci. Technol.* **50**, 12512–12520 (2016).
23. D. Zavala-Araiza *et al*., *Nat. Commun.* **8**, 14012 (2017).
24. D. R. Lyon *et al*., *Environ. Sci. Technol.* **50**, 4877–4886 (2016).
25. A. L. Mitchell *et al*., *Environ. Sci. Technol.* **49**, 3219–3227 (2015).
26. D. J. Zimmerle *et al*., *Environ. Sci. Technol.* **49**, 9374–9383 (2015).
27. T. Howard, T. W. Ferrara, A. Townsend-Small, *J. Air Waste Manag. Assoc.* **65**, 856–862 (2015).
28. R. A. Alvarez, D. R. Lyon, A. J. Marchese, A. L. Robinson, S. P. Hamburg, *Elem. Sci. Anth.* **4**, 000137 (2016).
29. A. J. Marchese *et al*., *Environ. Sci. Technol.* **49**, 10718–10727 (2015).
30. A. M. Fiore *et al*., *Geophys. Res. Lett.* **29**, 21-1–25-4 (2002).
31. Texas Commission on Environmental Quality (TCEQ), "Houston-Galveston-Brazoria Attainment Demonstration State Implementation Plan Revision for the 1997 Eight-Hour Ozone Standard" (2010), pp. 3–18; www.tceq.texas.gov/assets/public/implementation/air/sip/hgb/hgb_sip_2009/09017SIP_completeNarr_ado.pdf.
32. A. P. Ravikumar, J. Wang, A. R. Brandt, *Environ. Sci. Technol.* **51**, 718–724 (2017).
33. U.S. Department of Energy (DOE) Advanced Research Projects Agency – Energy, (ARPA-E, 2014), "ARPA-E MONITOR Program" (ARPA-E); https://arpa-e.energy.gov/?q=programs/monitor.
34. Environmental Defense Fund (EDF), "Methane Detectors Challenge" (EDF, 2014); www.edf.org/energy/natural-gas-policy/methane-detectors-challenge.
35. J. D. Albertson *et al*., *Environ. Sci. Technol.* **50**, 2487–2497 (2016).
36. D. J. Jacob *et al*., *Atmos. Chem. Phys.* **16**, 14371–14396 (2016).

ACKNOWLEDGMENTS

The authors are grateful to R. Harriss for support in the design and conduct of studies. We thank D. Zimmerle, A. Robertson, and A. Pintar for helpful discussions, and the scores of researchers that contributed to the body of work assessed here. **Funding:** Alfred P. Sloan Foundation, Fiona and Stan Druckenmiller, Heising-Simons Foundation, Bill and Susan Oberndorf, Betsy and Sam Reeves, Robertson Foundation, TomKat Charitable Trust, and the Walton Family Foundation (for EDF authors as well as support of related studies involving D.T.A, S.C.H., A.K., E.A.K., B.K.L., A.J.M., A.L.R., P.B.S., C.S., A.T.-S., S.C.W.); DOE National Energy Technology Laboratory (Z.R.B., K.J.D., T.L., A.L.R.); NASA Earth Science Division (D.J.J., E.A.K., J.D.M.); NOAA Climate Program Office (E.A.K., J.P., A.L.R., C.S.). **Author contributions:** R.A.A., D.Z-A., D.R.L., and S.P.H. conceived the study; R.A.A., D.Z-A., D.R.L., E.A.K., S.W.P. and S.P.H. designed the study and interpreted results with input from all authors; each author contributed to the collection, analysis, or assessment of one or more datasets necessary to perform this study; D.Z-A, D.R.L, and S.W.P, performed the analysis, with contributions from R.A.A., A.R.B., A.K., and M.O.; R.A.A., D.Z-A., D.R.L., S.W.P., S.C.W., and S.P.H. wrote the manuscript with input from all authors. **Competing interests**: None declared. **Data and materials availability:** All data and methods needed to reproduce the results in the paper are provided in the paper or as supplementary materials. Additional author disclosures (affiliations, funding sources, financial holdings) are provided in the supplementary materials.

SUPPLEMENTARY MATERIALS

www.sciencemag.org/content/361/6398/186/suppl/DC1
Materials and Methods
Additional Author Disclosures
Figs. S1 to S11
Tables S1 to S12
References (*37*–*77*)
Databases S1 and S2

19 December 2017; accepted 18 May 2018
Published online 21 June 2018
10.1126/science.aar7204

Science

Assessment of methane emissions from the U.S. oil and gas supply chain

Ramón A. Alvarez, Daniel Zavala-Araiza, David R. Lyon, David T. Allen, Zachary R. Barkley, Adam R. Brandt, Kenneth J. Davis, Scott C. Herndon, Daniel J. Jacob, Anna Karion, Eric A. Kort, Brian K. Lamb, Thomas Lauvaux, Joannes D. Maasakkers, Anthony J. Marchese, Mark Omara, Stephen W. Pacala, Jeff Peischl, Allen L. Robinson, Paul B. Shepson, Colm Sweeney, Amy Townsend-Small, Steven C. Wofsy and Steven P. Hamburg

Science **361** (6398), 186-188.
DOI: 10.1126/science.aar7204originally published online June 21, 2018

A leaky endeavor

Considerable amounts of the greenhouse gas methane leak from the U.S. oil and natural gas supply chain. Alvarez *et al.* reassessed the magnitude of this leakage and found that in 2015, supply chain emissions were ~60% higher than the U.S. Environmental Protection Agency inventory estimate. They suggest that this discrepancy exists because current inventory methods miss emissions that occur during abnormal operating conditions. These data, and the methodology used to obtain them, could improve and verify international inventories of greenhouse gases and provide a better understanding of mitigation efforts outlined by the Paris Agreement.

Science, this issue p. 186

ENVIRONMENTAL STUDIES

Quantifying methane emissions from the largest oil-producing basin in the United States from space

Yuzhong Zhang[1,2,3,4]*, Ritesh Gautam[2]*, Sudhanshu Pandey[5], Mark Omara[2], Joannes D. Maasakkers[5], Pankaj Sadavarte[5,6], David Lyon[2], Hannah Nesser[1], Melissa P. Sulprizio[1], Daniel J. Varon[1], Ruixiong Zhang[7,8], Sander Houweling[5,9], Daniel Zavala-Araiza[2,10], Ramon A. Alvarez[2], Alba Lorente[5], Steven P. Hamburg[2], Ilse Aben[5], Daniel J. Jacob[1]

Using new satellite observations and atmospheric inverse modeling, we report methane emissions from the Permian Basin, which is among the world's most prolific oil-producing regions and accounts for >30% of total U.S. oil production. Based on satellite measurements from May 2018 to March 2019, Permian methane emissions from oil and natural gas production are estimated to be 2.7 ± 0.5 Tg a^{-1}, representing the largest methane flux ever reported from a U.S. oil/gas-producing region and are more than two times higher than bottom-up inventory-based estimates. This magnitude of emissions is 3.7% of the gross gas extracted in the Permian, i.e., ~60% higher than the national average leakage rate. The high methane leakage rate is likely contributed by extensive venting and flaring, resulting from insufficient infrastructure to process and transport natural gas. This work demonstrates a high-resolution satellite data–based atmospheric inversion framework, providing a robust top-down analytical tool for quantifying and evaluating subregional methane emissions.

INTRODUCTION

Methane is a potent greenhouse gas with a relatively short average atmospheric residence time of about a decade and is also a precursor of tropospheric ozone (*1*). The emission-based radiative forcing for methane (including effects on tropospheric ozone and stratospheric water vapor) is 0.97 W m^{-2} since preindustrial times, which is about 60% of that for CO_2 (*2*). Roughly a third of the contemporary anthropogenic methane emissions come from the fossil fuel energy sector worldwide (oil, natural gas, and coal) (~100 to 180 Tg a^{-1}) (*3*, *4*, *5*). Curbing anthropogenic methane emissions, including those from the oil/gas sector, is considered an effective strategy to slow the rate of near-term climate warming (*1*). However, the rapid increase in oil and natural gas (O/G) production in the United States since around 2005, driven primarily by hydraulic fracturing and horizontal drilling, has led to major concerns about increasing methane emissions and adverse climate impacts (*6*). By upscaling data collected from field measurements in some of the largest O/G production basins in the United States, Alvarez *et al.* (*7*) estimated 13 Tg annual methane emissions from the national O/G supply chain for 2015, which is 60% higher than the official estimates by the U.S. Environmental Protection Agency (EPA) (*8*). The largest discrepancy was found in the O/G production segment where the estimate by Alvarez *et al.* (*7*) (7.6 Tg a^{-1}) was more than two times that by EPA, which relies on inventory-based estimates (3.5 Tg a^{-1}) (*8*).

While field measurements provide in-depth information about a particular site or area, it is often challenging to expand the measurement capacity to observe a diverse set of targets distributed globally over longer periods of time. Additional challenges exist for areas that are difficult to access for technical or proprietary reasons. On the other hand, global satellite observations of column atmospheric methane offer a unique vantage point to identify emission hot spots and quantify regional emissions (*9*). Using data from SCanning Imaging Absorption spectroMeter for Atmospheric CHartographY (SCIAMACHY) satellite observations averaged between 2003 and 2009, Kort *et al.* (*10*) found large anomalous methane levels from the Four Corners region in the United States, with total methane emissions associated with natural gas, coal, and coalbed sources estimated as 0.59 ± 0.08 Tg a^{-1}. While the SCIAMACHY data were fairly limited in spatial resolution (30 km × 60 km) and measurement precision [30 parts per billion in volume or (ppbv)] (*9*), it was the first time that satellite observations were used to quantify a dense O/G-related methane emission hot spot. This finding also led to several dedicated airborne studies to better understand methane sources in the region (*11*, *12*), which reported methane fluxes comparable to the satellite-based estimate (*10*).

Here, we demonstrate and exploit the capability of a recent spaceborne sensor, the Tropospheric Monitoring Instrument (TROPOMI), to map atmospheric methane enhancements in the United States and quantify emissions from the Permian Basin (Fig. 1), which has become one of the world's most prolific oil-producing regions in recent years due to advances in drilling technologies. Located in New Mexico and Texas in a region of ~400 km × 400 km, Permian is currently the largest oil-producing basin in the United States. In 2018, the Permian Basin produced 5.5 × 10^5 m^3 (or 3.5 million barrels) of crude oil and 3.2 × 10^8 m^3 (or 11 billion $feet^3$) of natural gas every day (~30 and ~10% of the U.S. national totals, respectively), which was 4 and 2.5 times their corresponding levels in 2007 (around the time of SCIAMACHY observations) (Fig. 2) (*13*). While the surging production in the Permian Basin and its importance in the U.S. oil boom during the last decade have been widely covered in mass

[1]School of Engineering and Applied Sciences, Harvard University, Cambridge, MA 02138, USA. [2]Environmental Defense Fund, Washington, DC 20009, USA. [3]School of Engineering, Westlake University, Hangzhou, Zhejiang Province, China. [4]Institute of Advanced Technology, Westlake Institute for Advanced Study, Hangzhou, Zhejiang Province, China. [5]SRON Netherlands Institute for Space Research, Utrecht, Netherlands. [6]TNO, Department of Climate, Air and Sustainability, Utrecht, Netherlands. [7]School of Earth and Atmospheric Sciences, Georgia Institute of Technology, Atlanta, GA 30332, USA. [8]ClimaCell Inc., 280 Summer Street Floor 8, Boston, MA 02210, USA. [9]Department of Earth Sciences, Vrije Universiteit Amsterdam, Amsterdam, Netherlands. [10]Institute for Marine and Atmospheric Research Utrecht (IMAU), Utrecht University, Utrecht, Netherlands.
*Corresponding author. Email: zhangyuzhong@westlake.edu.cn (Y.Z.); rgautam@edf.org (R.G.)

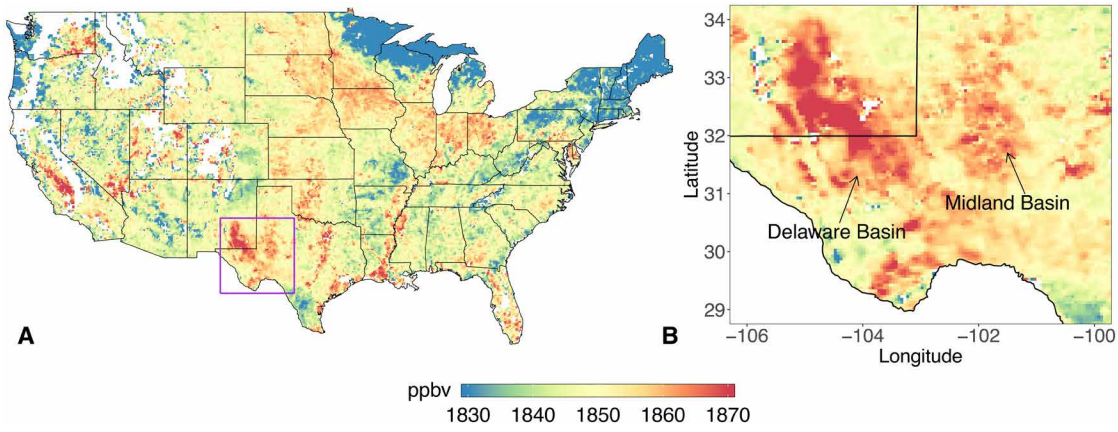

Fig. 1. Satellite observations of the Permian methane anomaly. TROPOMI satellite data derived elevation-corrected column methane mixing ratio for (**A**) the conterminous United States and (**B**) the Permian Basin containing the Delaware and Midland sub-basins. White shading represents missing data. Purple boundary in (A) indicates the study domain encompassing the Permian Basin. Methane averages are computed from monthly means of TROPOMI measurements during May 2018 and March 2019.

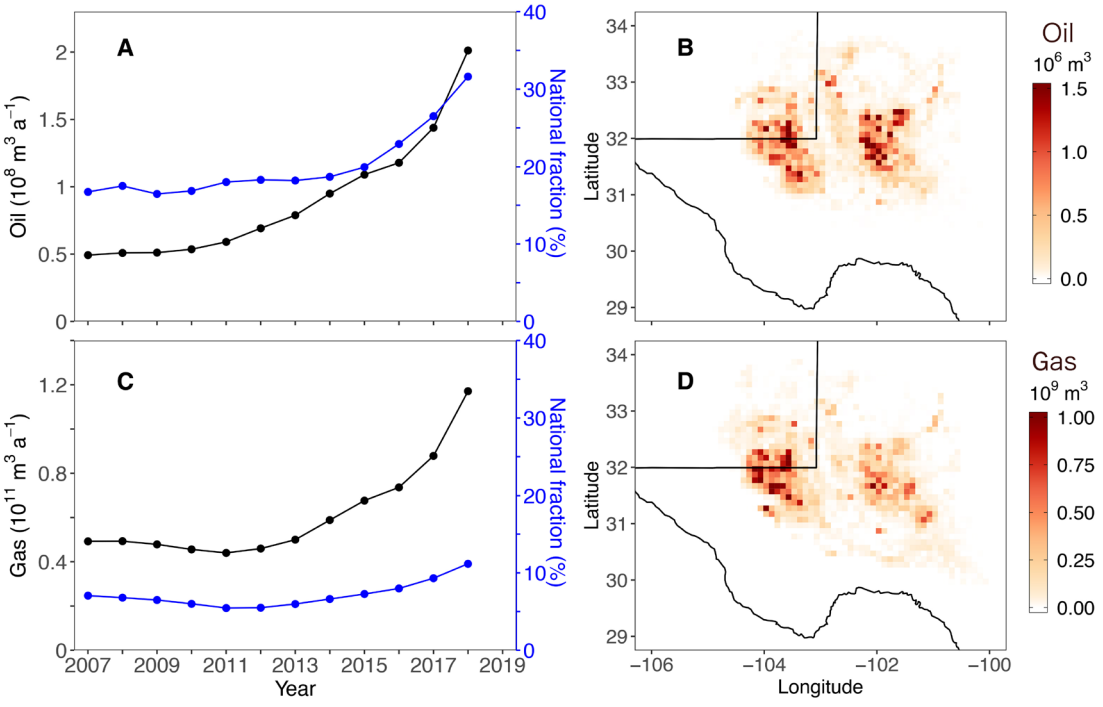

Fig. 2. Oil and gas production in the Permian Basin. (**A** and **C**) Time series of annual O/G production in black and the corresponding fractions of total U.S. production in blue [data from the Drilling Productivity Report by EIA (*13*)]. (**B** and **D**) Spatial distribution of oil and gas production for 2018 [data from Enverus Drillinginfo (*50*)]. Oil production includes both crude and condensate production. Gas production represents gross (before processing) gas production.

media (*14*), the scale of associated methane emissions from this critical O/G basin is unknown, despite reports of increased flaring and venting activity (*15*).

Using 11 months of recent data acquired by TROPOMI during 2018–2019, we focus on the distinct methane concentration anomaly over the Permian Basin and quantify the associated methane emissions with a state-of-the-art atmospheric inverse modeling framework. TROPOMI was launched in October 2017 onboard the European Space Agency's Sentinel-5P satellite and provides column atmospheric methane measurements with higher spatial resolution (7 km × 7 km at nadir) and precision (0.6%) than was previously available (*16*), providing near-daily global coverage with its large 2600-km-wide swath (*17*). Our integrated satellite-based approach provides new insights into the dynamic landscape of O/G-related methane emissions in the United States and should pave the way forward toward routine quantification, monitoring, and evaluation of methane emissions from source regions distributed globally.

RESULTS

Satellite observations of the Permian methane anomaly

Figure 1A shows a map of column-averaged dry-air methane mixing ratio over the conterminous United States, retrieved from TROPOMI measurements, with correction for the topography effect (denoted

as XCH_4^t; see Materials and Methods). The data are averaged from May 2018 to March 2019. Substantial enhancements of XCH_4^t relative to the surrounding background, up to ~30 ppbv, are found over the Permian Basin, indicating strong methane emissions. Other notable enhancements are observed in California's central valley, coastal Southeast, and the Mississippi River Valley, likely associated with anthropogenic (agriculture, dairy) and natural (wetland) sources. The elevated methane levels in central California were also seen earlier in the SCIAMACHY analysis (*10*).

The methane enhancements over the Permian Basin show a characteristic two-branch pattern, which aligns with the two major O/G production sub-basins, the Delaware basin to the west and the Midland basin to the east (Fig. 1B). The enhancement over the Delaware basin, where extensive new exploitation has taken place during the last 5 years (*18*) (fig. S1), is larger than that over the Midland basin (Fig. 1B). Intensive O/G production activity in these two sub-basins is also captured by satellite observations of radiant heat from gas flaring [Fig. 3A; nighttime observations by the Visible Infrared Imaging Radiometer Suite (VIIRS)] a nd NO_2 tropospheric column densities (Fig. 3B; daytime observations by TROPOMI). Flaring is a common practice in O/G operations to burn off unwanted or excess gas, and NO_2 is a gaseous pollutant released during gas flaring and other combustion activities in O/G fields (*19*, *20*). On the basis of measurements by the VIIRS instrument onboard the Suomi National Polar-orbiting Partnership satellite, we estimate an average flaring rate of 5.9 ± 1.2 billion m^3 a^{-1} during the period of this study, about 4.6% of the gross gas production (see text S1). A fourfold increase in flaring intensity since 2012, observed by the VIIRS instrument, is indicative of the rapid growth in O/G production across the Permian Basin (fig. S1).

Methane emission quantification

We quantify the methane emission rate from the Permian Basin and its spatial distribution with atmospheric inverse modeling, which optimizes spatially resolved methane emission rates by drawing information from TROPOMI observations and the prior emission estimate following the Bayesian rule. The inversion seeks to optimize monthly methane emission rates resolved at 0.25° × 0.3125° horizontal resolution in a study domain containing the Permian Basin and the surrounding region (29°–34°N, 100°–106°W). The solution to the optimization is found analytically with closed-form characterization of the error statistics (*3*). An atmospheric transport model (a nested version of GEOS-Chem over North America with a 0.25° × 0.3125° horizontal resolution) (*21*) is used as the forward model to relate atmospheric methane columns with ground-level emissions in the study domain and the contributions from outside the domain. The optimization by the inversion significantly reduces the observation-model mismatch with decreased root mean square error (prior, 23 ppbv; posterior, 14 ppbv) and increased correlation (*R*; prior, 0.30; posterior, 0.62) (fig. S2). See Materials and Methods for more details about the configurations of the inverse modeling including error accounting and prior information.

When aggregating monthly spatially resolved posterior emissions to the basin-level annual average, we find a methane emission flux of 2.9 ± 0.5 Tg a^{-1} from the Permian Basin (30°–34°N, 101°–105°W) (Fig. 4A; see Materials and Methods for the uncertainty analysis). This estimate is more than a factor of 2 larger than the bottom-up estimate based on an extrapolation of EPA greenhouse gas inventory data (EI_{BU}, 1.2 Tg a^{-1}; see Materials and Methods) (Fig. 4A), suggesting that current methane emissions in the Permian are underrepresented in national bottom-up emission inventories (*22*). Our inversion result is in close agreement with a basin-level estimate based on extrapolation of limited ground-based site-level measurements in the Permian (EI_{ME}, 2.8 Tg a^{-1}) (Fig. 4A). It should be noted that these site-level measurements were primarily conducted in the New Mexico portion of the Permian Basin and covered only a

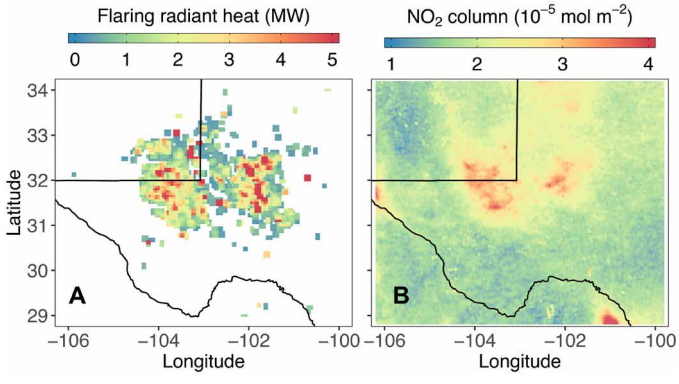

Fig. 3. Satellite observations of gas flaring radiant heat and NO_2 tropospheric column density over the Permian Basin. (**A**) Gas flaring radiant heat is the annual average of 2018 measured by the VIIRS satellite instrument, and (**B**) NO_2 tropospheric column density is the 3-month average (June, July, and August of 2018) measured by the TROPOMI instrument, indicating colocated hot spots over the Delaware and Midland sub-basins.

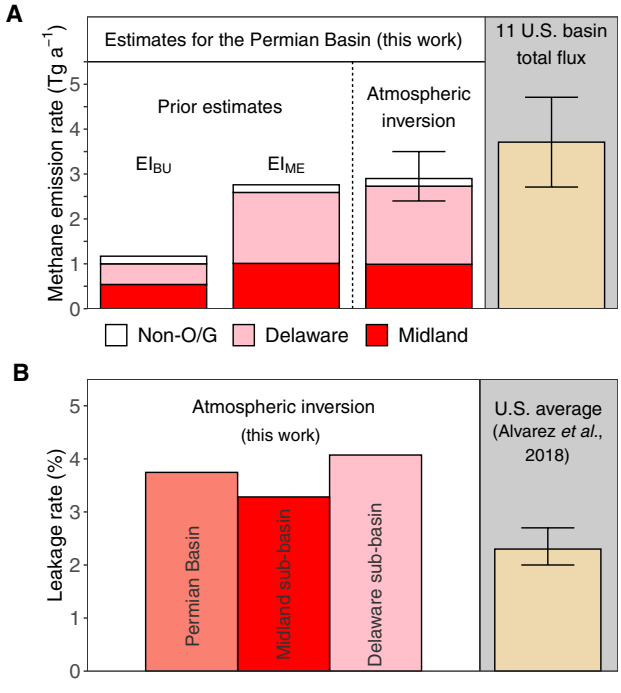

Fig. 4. Methane emission quantification for the Permian Basin. (**A**) Annual methane emissions from the Permian Basin from two prior emission inventories (EI_{BU} and EI_{ME}), and TROPOMI satellite data–based atmospheric inversion and a mass balance method. The breakdown for Delaware, Midland, and non-O/G sources is shown in pink, red, and white for EI_{BU}, EI_{ME}, and atmospheric inversion, respectively. The estimate for the Permian Basin is compared with total emissions from 11 U.S. basins reported in literature (*7*, *24*, *25*) (table S1). (**B**) Leakage rates for the Permian Basin and two sub-basins, in comparison with the average leakage reported for the entire United States (*7*).

small fraction of production sites (see Materials and Methods and text S2). As a comparison, we also apply a fast mass balance method following Buchwitz *et al.* (*23*) to estimate basin-level emissions, which yields an annual mean emission rate of 3.2 ± 2.0 Tg a^{-1} for the Permian Basin. This result is consistent with that derived from a full atmospheric inversion. Despite the large uncertainty of the mass balance method, this data-driven approach provides an independent estimate of emissions derived primarily using TROPOMI data (see text S3 for more discussion).

Removing the non-O/G sources (0.2 Tg a^{-1}) from the total flux obtained via the inversion (2.9 Tg a^{-1}), we estimate the methane emissions related to O/G activity to be 2.7 Tg a^{-1} in the Permian Basin. Put in the context of national emissions, this value is approximately one quarter of total emissions from all U.S. oil and gas production areas in 2015 (10.9 Tg a^{-1}, including emissions from production, gathering, and processing, which largely occur in the production areas) (*7*). Our estimated emission rate for the Permian is significantly higher than those reported in the literature for other major U.S. O/G-producing basins. Table S1 summarizes methane emission estimates for 11 U.S. basins (*7*, *24*, *25*) from previous aircraft-based studies [i.e., Haynesville (*24*, *26*), Barnett (*24*, *27*), Northeast Pennsylvania (*26*, *28*), Southwest Pennsylvania (*25*), San Juan (*12*), Fayetteville (*26*, *29*), Bakken (*24*, *30*), Uinta (*31*), Weld (*32*), West Arkoma (*26*), Eagle Ford (*24*), and the Denver Basin (*24*)]. Our estimate for the Permian (2.7 Tg a^{-1}) is about a factor of 4 higher than the largest methane emissions from these previously reported O/G basins [i.e., Eagle Ford, 0.73 Tg a^{-1} (*24*)] and is even comparable to the 11-basin sum (3.7 Tg a^{-1}) (Fig. 4A and table S1). This comparison with recent literature indicates that the Permian Basin is likely the largest observed methane-emitting O/G basin in the United States and a substantial contributor to national O/G-related emissions.

Distribution of methane emissions

High-resolution observations from TROPOMI enable us to resolve methane emissions at an unprecedented spatial and temporal resolution, relative to the previous generation of satellite instruments such as the Greenhouse gases Observing SATellite (GOSAT) and SCIAMACHY (*9*). Figure 5 presents the spatial distribution of methane emissions in the Permian Basin at about a quarter-degree resolution derived from our atmospheric inversion. Compared to the prior inventory EI_{BU}, our inversion finds larger methane emissions near the center of the Delaware and Midland sub-basins. Sensitivity inversions further show that this spatial pattern is robust against prior emissions of varied magnitudes and distributions (fig. S3), demonstrating that it is primarily informed by satellite observations.

The spatial distribution of methane emissions derived from inversion is closely correlated with that of gross gas production (R = 0.78), but to a lesser degree with that of oil production (R = 0.53) and that of the well number density (R = 0.31) (fig. S4). Similarly, when we sum up the O/G-related emissions for two sub-basins, the ratio of methane emissions between Delaware and Midland (1.7/1.0 Tg a^{-1} = 1.7) is closest to the ratio of gas production (1.4), compared to that of oil production (1.0) and well number density (0.7). Because unconventional wells tend to have much higher production per well than conventional wells (*33*), the dependence of methane emissions on gross gas production rather than the well number density suggests that unconventional wells and infrastructure associated with these wells (e.g., gathering stations), which have been developed recently, are likely the major methane emitters in the Permian Basin.

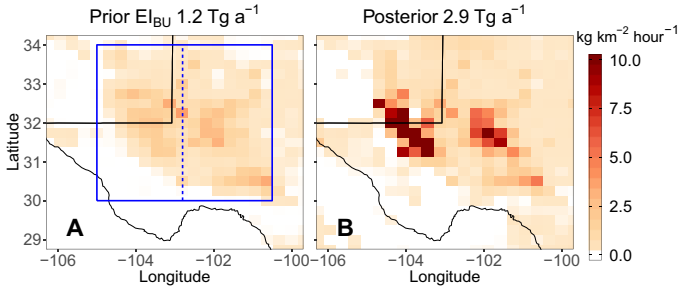

Fig. 5. Spatial distribution of methane emission rates in the Permian Basin. (**A**) Bottom-up emission inventory EI_{BU} extrapolated from EPA greenhouse gas inventory data (prior). (**B**) TROPOMI observation–derived emissions using Bayesian atmospheric inverse modeling (posterior). The prior and posterior basin-total emissions, indicated on top of the figure, are computed over the area enclosed by the solid blue boundary, with contributions from two sub-basins, the Delaware (left of the dashed line) and Midland (right of the dashed line).

In addition to the spatial distribution, our monthly inversion also provides information about the temporal variation of methane emissions during the 11 months of observation (fig. S5). Although the inversion's ability to resolve the spatial distribution of emissions varies from month to month because of uneven monthly sampling of TROPOMI (fig. S5), our inversion ensemble (table S2 and fig. S5) generally results in consistent monthly basin-level emission estimates (see also uncertainty analysis in Materials and Methods). We speculate that high emissions in December 2018 may be related to a very low in-basin gas price toward the end of 2018, resulting from insufficient gas gathering and transmission capacity in the Permian Basin (*33*,*34*). That said, we do not find an apparent increasing trend in methane emissions, although natural gas production from the Permian Basin increased steadily by ~20% during the overlapping 11-month period (fig. S6). Further investigation is required to delineate factors controlling the temporal variations of O/G-related methane emissions.

DISCUSSION

Using an inverse analysis of TROPOMI satellite observations, we estimate a total methane flux of 2.9 ± 0.5 Tg a^{-1} in the Permian Basin, with 2.7 Tg a^{-1} coming from O/G-related activity. Methane losses of this magnitude represent a waste of an important resource; for instance, this is enough natural gas to supply 7 million households in the state of Texas (*35*). Moreover, the 2.7 Tg a^{-1} methane emitted in Permian results in the same radiative forcing as ~260 Tg a^{-1} CO_2 over a 20-year time horizon (86 Tg CO_2 a^{-1} over a 100-year time horizon) (global warming potential of 96 for 20 years and 32 for 100 years) (*7*, *36*), about the same as annual CO_2 emissions from the entire U.S. residential sector (290 Tg CO_2 a^{-1} in 2017) (*22*).

Our estimate (2.7 Tg a^{-1}) equates to a production-normalized (73 Tg CH_4 a^{-1}, derived from 127 m^3 a^{-1} natural gas production during the study period using 80% methane content by volume) emission rate (or methane leakage rate) of 3.7 ± 0.7%, which is ~60% higher than the national average of 2.3 ± 0.3% (*7*) (Fig. 4B). The leakage rate is even higher for the rapidly developing Delaware sub-basin (4.1%). Comparable high leakage rates have also been reported in other oil production–focused basins such as the Bakken (*24*) (table S1), but these basins produce much lower natural gas than the Permian Basin does. Previous studies summarized in table

S1 show an inverse relationship between the basin-level leakage rate and gas production (*24*); however, the Permian Basin is an outlier with high oil production, high gas production, and a high leakage rate.

Overall, the high leakage rate in the Permian Basin appears to be associated with insufficient infrastructure for natural gas gathering, processing, and transportation (*34*, *37*), leading to extensive venting and flaring (Fig. 3), which contributes to high methane emissions. The greater profitability of oil production contributes to a lack of investment in natural gas takeaway capacity, which, in turn, has resulted in excessive supply of associated gas and a very low in-basin gas price in the Permian (*34*). In addition, with the rescinding of U.S. federal requirements on gas capture and fugitive emissions in 2018, current regulations on O/G methane emissions in the Permian Basin are less stringent at both federal and state levels (see text S4). All these factors may increase the incentive for operators to vent and flare their product. On the other hand, the higher-than-average leakage rate in the Permian Basin implies an opportunity to reduce methane emissions in this rapidly growing oil and gas–producing region, through better design, effective management, regulation, and infrastructure development.

MATERIALS AND METHODS

TROPOMI methane observations

We use daily column-averaged dry air column methane mixing ratio (XCH_4) data retrieved from TROPOMI measurements (*38*) between May 2018 and March 2019. TROPOMI, onboard the polar-orbiting Sentinel-5 Precursor satellite, is a push-broom imaging spectrometer that provides near-daily global coverage with a swath width of 2600 km and a nadir ground pixel size of 7 km × 7 km at approximately 13:30 local overpass time (*17*). The retrieval algorithm accounts for the "full physics" of the light path by simultaneously inferring methane concentrations and physical scattering properties, using the oxygen A-band in the near infrared (NIR) and the methane absorption band in the short-wave infrared (SWIR) (*39*). Only high-quality XCH_4 measurements retrieved under cloud-free conditions are used in this study (as indicated by the retrieval quality assurance flags in TROPOMI data product). These measurements are filtered for solar zenith angle (<70°), low viewing zenith angle (<60°), smooth topography (1 SD of surface elevation <80 m within 5-km radius), and low aerosol load (aerosol optical thickness <0.3 in NIR) (*40*).

The TROPOMI XCH_4 product is further corrected for any known retrieval biases (*40*). The errors in the TROPOMI XCH_4 measurements have been assessed against GOSAT XCH_4 data (*38*) and were found to correlate with surface albedo. A global bias correction linearly dependent on surface albedo was then derived and applied to the TROPOMI data (*40*). This bias-corrected TROPOMI XCH_4 product is used in this study. Negligible correlation of errors with other retrieved parameters (e.g., aerosol optical thickness) was found in the assessment. Validation with independent ground-based measurements from the Total Column Carbon Observing Network shows that the bias-corrected TROPOMI XCH_4 has a bias of −4.3 ± 7.4 ppbv, improved upon the uncorrected XCH_4 product (−12 ± 11.5 ppbv) (*40*). In addition, we also examine the correlation between bias-corrected XCH_4 and other retrieved parameters for the subset of TROPOMI data over the domain of this study. We find no correlation with albedo (R^2 = 0.00) and a negligible correlation with aerosol optical thickness (R^2 = 0.07), supporting the idea that the XCH_4 enhancement over the Permian Basin (Fig. 1B) is robust.

Figure S7A shows the average XCH_4 over the conterminous United States and the Permian Basin between May 2018 and March 2019 before the topographical correction. We derive the elevation-corrected methane column (XCH_4^t) shown in Fig. 1 by applying a third-order polynomial correction fitted over the U.S. domain following Kort *et al.* (*10*). The mass balance method uses the elevation-corrected data (XCH_4^t) for emission quantification, while the inversion method uses XCH_4 (bias-corrected) directly obtained from the data product, because the topography effect is taken care of by the atmospheric transport model.

Atmospheric inverse modeling

We perform an inverse analysis of TROPOMI observations to derive optimized estimation of monthly methane emissions at 0.25° × 0.3125° horizontal resolution in the Permian Basin. Quantification of emissions at this combination of relatively high spatial and temporal resolution, not achievable with previous generations of satellite observations such as from GOSAT or SCIAMACHY, is enabled by higher-resolution TROPOMI satellite observations (*41*). Figure S7B shows that the Permian Basin is well sampled by TROPOMI during the study period, likely because of frequent cloud-free conditions in the region. A total of ~200,000 TROPOMI XCH_4 retrievals within the study domain (29°–34°N, 100°–106°W) between May 2018 and March 2019 are used for the inversion.

Let $\boldsymbol{x}$ be the state vector that we seek to optimize through inversion, including a gridded ensemble of methane emissions and an additional element representing the regional model bias in XCH_4. The regional model bias term (a monthly scalar uniform over the inversion domain) is necessary to account for spatially uniform biases caused by imperfect lateral boundary condition and emission errors outside the study domain. The inversion solves for an optimal estimate of $\boldsymbol{x}$ by minimizing the following cost function

$$J(\boldsymbol{x}) = (\boldsymbol{x} - \boldsymbol{x}_A)^T \mathbf{S}_A^{-1} (\boldsymbol{x} - \boldsymbol{x}_A) + (\boldsymbol{y} - \mathbf{K}\boldsymbol{x})^T \mathbf{S}_O^{-1} (\boldsymbol{y} - \mathbf{K}\boldsymbol{x}) \quad (1)$$

where TROPOMI XCH_4 observations are assembled in $\boldsymbol{y}$, $\boldsymbol{x}_A$ is the prior estimate of $\boldsymbol{x}$, $\mathbf{S}_A$ is the prior error covariance matrix, $\mathbf{S}_O$ is the observational error covariance matrix, and $\mathbf{K}$ is the Jacobian matrix describing the sensitivity of XCH_4 to emissions and the regional model bias ($\partial\boldsymbol{y}/\partial\boldsymbol{x}$).

Minimization of Eq. 1 at $\nabla_{\boldsymbol{x}} J(\boldsymbol{x}) = 0$ yields the posterior estimation ($\hat{\boldsymbol{x}}$), the posterior error covariance matrix ($\hat{\mathbf{S}}$), and the averaging kernel matrix ($\mathbf{A}$) (*42*)

$$\hat{\boldsymbol{x}} = \boldsymbol{x}_A + \mathbf{S}_A \mathbf{K}^T (\mathbf{K}\mathbf{S}_A\mathbf{K}^T + \mathbf{S}_O)^{-1} (\boldsymbol{y} - \mathbf{K}\boldsymbol{x}_A) \quad (2)$$

$$\hat{\mathbf{S}} = (\mathbf{K}^T \mathbf{S}_O^{-1} \mathbf{K} + \mathbf{S}_A^{-1})^{-1} \quad (3)$$

$$\mathbf{A} = \mathbf{I}_n - \hat{\mathbf{S}}\mathbf{S}_A^{-1} \quad (4)$$

Here, $\mathbf{I}_n$ is an identity matrix where n is the dimension of the state vector $\boldsymbol{x}$. The trace of $\mathbf{A}$, often called as the degrees of freedom for signal (DOFS), quantifies the number of pieces of information constraining the n-dimensional state vector.

To solve for Eqs. 2 to 4, the prior estimate ($\boldsymbol{x}_A$) for gridded methane emissions is required. Using different sources of information, we create two gridded emission inventories for the study region: one based on bottom-up information (EI_{BU}) and the other based on extrapolation

of ground-based site-level measurements (EI_{ME}) (see below for descriptions of the inventories). Both emission inventories are time invariant. We use EI_{BU} as the prior estimate in the base inversion, while we use EI_{ME} in a sensitivity inversion to evaluate the impact of the prior estimate (PI_EI_{ME}; see table S2). We perform further evaluations using prior emissions constructed by disaggregating the total O/G-related emission flux from EI_{BU} with varied spatial proxies (i.e., well count, PI_EI_{well}, natural gas production, PI_EI_{gas}, and oil production, PI_EI_{oil}) (table S2 and fig. S3).

The difference between the EI_{BU} and EI_{ME} (Fig. 5A and fig. S3A) measures the uncertainty of our prior knowledge, and we thus specify prior errors ($\mathbf{S}_A$) for emissions as the absolute difference between EI_{BU} and EI_{ME}. We also specify the prior error for the regional model XCH_4 bias as 10 ppbv. To test the sensitivity to prior errors, we perturb $\mathbf{S}_A$ in two sensitivity inversions by doubling (PE × 2) or halving (PE × 0.5) prior errors (table S2). $\mathbf{S}_O$ is constructed with the residual error method (*43*), which results in an error averaged at ~11 ppbv. Both $\mathbf{S}_O$ and $\mathbf{S}_A$ are taken to be diagonal matrices. We also perform a sensitivity inversion to test the impact of error correlations with off-diagonal terms specified following Cusworth *et al.* (*44*) (OE_Cor; see table S2).

A nested version of the GEOS-Chem chemical transport model (12.1.0) is used as the forward model in the inversion to link XCH_4 to surface emissions. To account for the vertical sensitivity of the satellite instrument, we compute simulated XCH_4 by applying TROPOMI averaging kernels to simulated methane vertical profiles. We construct the Jacobian matrix $\mathbf{K}$, column by column, with simulations perturbing each state vector element independently. The simulations are performed over North America and adjacent oceans driven by GEOS-FP–assimilated meteorological data from the NASA Global Modeling and Assimilation Office on a 0.25° × 0.3125° horizontal grid and 47 vertical layers (~30 layers in the troposphere) (*21*). The boundary conditions for the nested-grid simulation are from a 4° × 5° global simulation from May 2018 to March 2019 driven by GEOS-FP meteorological fields. Note that methane emissions and sinks used in this simulation are optimized with previous-year (2010–2017) GOSAT satellite data following Maasakkers *et al.* (*3*). Such generated boundary conditions may be biased (i.e., unable to capture the growth of global methane concentrations; see fig. S9), and we account for it by introducing a monthly regional model bias term in the inversion. The retrieved regional model biases may vary with the extent of the inversion domain. To test this sensitivity, we also perform an inversion with a larger spatial domain (27°–36°N, 98°–108°W) (Bg_Large; see table S2).

Inversion uncertainty

The posterior error covariance matrix ($\hat{\mathbf{S}}$, Eq. 2) and averaging kernel matrix ($\mathbf{A}$, Eq. 3) evaluate the uncertainty of an inversion solution given inversion parameters (e.g., $\mathbf{S}_A$, $\mathbf{S}_O$, forward model). Figure S5 shows monthly posterior errors for basin-level emissions (derived from $\hat{\mathbf{S}}$) and corresponding DOFS (trace of $\mathbf{A}$) from our base inversion. Overall, the posterior errors for basin-level emissions are <5% of the estimated emission flux, and the DOFS are between 5 and 30 for the monthly inversion, indicating that the TROPOMI data are able to constrain basin-level methane emissions and partially resolve the spatial distribution on a monthly basis. The monthly variations in the posterior error and DOFS are mainly driven by uneven data coverage from TROPOMI sampling. For example, poor data coverage in November 2018 results in a large posterior error and a small DOFS (fig. S5).

We also perform an ensemble of sensitivity inversions by perturbing the configurations and parameters in the base inversion (table S2), aiming to characterize the uncertainties resulting from assumptions made in the inversion not captured by the analytical posterior error. Our results show that all these sensitivity inversions lead to consistent basin-level emission estimates. Annual mean fluxes from sensitivity inversions are within 0.5 Tg a^{-1} of that from our base inversion (table S2), with general agreement in monthly variations as well (fig. S5). Because the uncertainty resulting from sensitivity inversions are significantly larger than that deduced from posterior error covariance matrix (fig. S5), we report the uncertainty of our basin-level emission estimate (0.5 Tg a^{-1}) as half of the range from the inversion ensemble (2.4 to 3.4 Tg a^{-1}).

Furthermore, to assess the uncertainty due to model transport, we compare hourly GEOS-FP 10-m wind speed against measurements at the Midland Airport (MAF) in the Permian Basin during the period of May 2018 and March 2019. Airport wind measurements are not assimilated in the GEOS-FP reanalysis (*45*), so these observations are independent. We find that the GEOS-FP 10-m wind speed compares well with the airport measurements in both daytime and nighttime (fig. S8), with mean biases of less than 6% in the mean wind speed. We conclude that errors in the model wind fields are unlikely to be a major source of error in the inversion.

We introduced a regional model bias term in monthly inversions to correct for regional background biases in simulated methane concentrations, which result mainly from imperfect boundary conditions. To check our estimate for this regional bias term, we sample the model simulation to compare with independent observations, i.e., surface measurements at the Mauna Loa Observatory (MLO; a Pacific free tropospheric site upwind of the North American continent) (*46*), tower measurements at Moody, Texas (WKT) (*47*), and aircraft measurements offshore Corpus Christi, Texas (TGC) (*48*). The latter two sites are geographically much closer to the Permian Basin (~400 km from WKT and ~700 km from TGC) than MLO, but can be affected by local emissions that are not optimized in our inversion. Our results show that the model simulation, when corrected with monthly regional model biases (derived from monthly inversions over the Permian Basin), is able to capture the observed monthly variation in methane concentrations, notably the sharp increase from August to October 2018 in MLO and WKT observations (fig. S9), supporting that it is necessary to optimize the regional model bias in the inversion. Better agreement is observed at MLO and TGC compared to WKT (fig. S9), likely because WKT is located closer to local sources that are not fully optimized in the inversion. Overall, most of the differences between the prior simulation and TROPOMI observations can be explained by the regional model biases, except for the mismatch in the vicinity of the Permian Basin (fig. S2). We further perform a sensitivity inversion with a varied spatial domain (Bg_Large). Compared to the base inversion, Bg_Large results in a lower regional methane background (by 3 ppbv on average) and a higher methane emission flux (3.4 Tg a^{-1}) (table S2 and fig. S5), reflecting the error correlation between regional methane biases and methane emissions.

In addition, we note that the inversion cannot fully explain the methane enhancement extending outside the Delaware Basin in the northwest direction (near 33°N, 105°W), although the inversion overall substantially improves the agreement between observations

and model simulations (fig. S2). While our investigations do not attribute an obvious source of emissions causing the northwestern enhancement (whether oil/gas or other sources), the basin-level O/G emission estimates presented here are robust if this enhancement is caused by non-O/G sources, but are conservative if it is caused by O/G sources.

Emission inventory based on bottom-up information

We create a bottom-up methane emission estimate (EI_{BU}) for the study domain starting from the gridded version of the EPA anthropogenic greenhouse gas emission inventory for 2012 (*49*). Maasakkers *et al.* (*49*) developed a procedure to spatially and temporally allocate the national sectorial methane emissions reported in the U.S. Inventory of Greenhouse Gas Emissions and Sinks (GHGI) by U.S. EPA on a 0.1° × 0.1° grid, using various databases at the state, county, local, and point-source level. The emission inventory includes methane emissions from agriculture, coal mining, natural gas systems, petroleum (oil) systems, waste, and other minor anthropogenic sources.

To reflect the intensifying exploitation activity in recent years in the Permian Basin, we then make an extrapolation of the methane emissions from the oil and gas production sector, using 2018 Enverus Drillinginfo data on well count, well completion, and production (*50*). To account for the changes in the national average emission factors, we further scale the subsectorial production emissions using the ratio between the latest GHGI (*22*) and a previous GHGI that Maasakkers *et al.* (*49*) was based on (*51*) for 2013 emissions. The updates result in total methane emissions of 1.2 Tg a^{-1} in the Permian Basin (blue box in Fig. 5A), with 1.0 Tg a^{-1} coming from O/G-related emissions and the remainder mainly from agriculture. We use this updated gridded emission inventory (EI_{BU}) as the prior emission estimate for the inversion. The resulting emissions inventory dataset (EI_{BU} inventory) is publicly available for our study region encompassing the entire Permian Basin (https://doi.org/10.7910/DVN/NWQGHU).

Emission inventory based on site-level emission measurements

An alternative prior estimation of methane emissions is obtained by extrapolating ground-based methane emission measurements from a limited sample of oil and gas production sites in the Permian Basin (primarily in the New Mexico portion of the basin) during July and August 2018 (*52*). The measurements found a wide range of site-level emission rates, which appear to be associated with the complexity of infrastructure, and were classified into emission rates for simple (with only wellheads and/or pump jacks) versus complex sites (also with storage tanks and/or compressors). Extrapolating these site-level emission rates to the entire Permian gave a basin-level methane emission rate of 2.3 Tg a^{-1} from O/G production. Additional emissions from compressor stations and processing plants are estimated to be 0.22 and 0.14 Tg a^{-1}, respectively, using activity data from Enverus Drillinginfo's midstream infrastructure dataset, facility-level emission factors from literature (*53*, *54*), and blowdown event emission factors from GHGI (*22*). We then disaggregate the basin-level O/G-related emissions to a 0.1° × 0.1° grid by the spatial distribution of gas production (Fig. 2D). To complete the inventory, non-O/G anthropogenic methane emissions (0.2 Tg a^{-1}) are taken from EI_{BU}. This emission inventory (EI_{ME}), based primarily on extrapolation of limited site-level measurements, provides an alternative prior estimate for the inversion and is used to test the sensitivity of the results to the choice of prior information (fig. S3). See text S2 for detailed information regarding the site-level measurements and the extrapolation procedure. The resulting emissions inventory dataset (EI_{ME} inventory) is publicly available for our study region encompassing the entire Permian Basin (https://doi.org/10.7910/DVN/NWQGHU).

SUPPLEMENTARY MATERIALS

Supplementary material for this article is available at http://advances.sciencemag.org/cgi/content/full/6/17/eaaz5120/DC1

REFERENCES AND NOTES

1. D. Shindell, J. C. I. Kuylenstierna, E. Vignati, R. van Dingenen, M. Amann, Z. Klimont, S. C. Anenberg, N. Muller, G. Janssens-Maenhout, F. Raes, J. Schwartz, G. Faluvegi, L. Pozzoli, K. Kupiainen, L. Höglund-Isaksson, L. Emberson, D. Streets, V. Ramanathan, K. Hicks, N. T. K. Oanh, G. Milly, M. Williams, V. Demkine, D. Fowler, Simultaneously mitigating near-term climate change and improving human health and food security. *Science* **335**, 183–189 (2012).
2. G. Myhre, D. Shindell, F.-M. Bréon, W. Collins, J. Fuglestvedt, J. Huang, D. Koch, J.-F. Lamarque, D. Lee, B. Mendoza, T. Nakajima, A. Robock, G. Stephens, T. Takemura, H. Zhang, Anthropogenic and natural radiative forcing, in *Climate Change 2013: The Physical Science Basis. Contribution of Working Group I to the Fifth Assessment Report of the Intergovernmental Panel on Climate Change,* T. F. Stocker, D. Qin, G.-K. Plattner, M. Tignor, S. K. Allen, J. Boschung, A. Nuales, Y. Xia, V. Bex, P. M. Midgley, Eds. (Cambridge Univ. Press, 2013), pp. 659–740.
3. J. D. Maasakkers, D. J. Jacob, M. P. Sulprizio, T. R. Scarpelli, H. Nesser, J.-X. Sheng, Y. Zhang, M. Hersher, A. A. Bloom, K. W. Bowman, J. R. Worden, G. Janssens-Maenhout, R. J. Parker, Global distribution of methane emissions, emission trends, and OH concentrations and trends inferred from an inversion of GOSAT satellite data for 2010–2015. *Atmos. Chem. Phys.* **19**, 7859–7881 (2019).
4. S. Schwietzke, O. A. Sherwood, L. M. P. Bruhwiler, J. B. Miller, G. Etiope, E. J. Dlugokencky, S. E. Michel, V. A. Arling, B. H. Vaughn, J. W. C. White, P. P. Tans, Upward revision of global fossil fuel methane emissions based on isotope database. *Nature* **538**, 88–91 (2016).
5. B. Hmiel, V. V. Petrenko, M. N. Dyonisius, C. Buizert, A. M. Smith, P. F. Place, C. Harth, R. Beaudette, Q. Hua, B. Yang, I. Vimont, S. E. Michel, J. P. Severinghaus, D. Etheridge, T. Bromley, J. Schmitt, X. Faïn, R. F. Weiss, E. Dlugokencky, Preindustrial $^{14}CH_4$ indicates greater anthropogenic fossil CH_4 emissions. *Nature* **578**, 409–412 (2020).
6. R. A. Alvarez, S. W. Pacala, J. J. Winebrake, W. L. Chameides, S. P. Hamburg, Greater focus needed on methane leakage from natural gas infrastructure. *Proc. Natl. Acad. Sci. U.S.A.* **109**, 6435–6440 (2012).
7. R. A. Alvarez, D. Zavala-Araiza, D. R. Lyon, D. T. Allen, Z. R. Barkley, A. R. Brandt, K. J. Davis, S. C. Herndon, D. J. Jacob, A. Karion, E. A. Kort, B. K. Lamb, T. Lauvaux, J. D. Maasakkers, A. J. Marchese, M. Omara, S. W. Pacala, J. Peischl, A. L. Robinson, P. B. Shepson, C. Sweeney, A. Townsend-Small, S. C. Wofsy, S. P. Hamburg, Assessment of methane emissions from the U.S. oil and gas supply chain. *Science* **361**, 186–188 (2018).
8. EPA, Inventory of US greenhouse gas emissions and sinks: 1990–2015 (2017); https://www.epa.gov/ghgemissions/inventory-us-greenhouse-gas-emissions-and-sinks-1990-2015.
9. D. J. Jacob, A. J. Turner, J. D. Maasakkers, J. Sheng, K. Sun, X. Liu, K. Chance, I. Aben, J. McKeever, C. Frankenberg, Satellite observations of atmospheric methane and their value for quantifying methane emissions. *Atmos. Chem. Phys.* **16**, 14371–14396 (2016).
10. E. A. Kort, C. Frankenberg, K. R. Costigan, R. Lindenmaier, M. K. Dubey, D. Wunch, Four corners: The largest US methane anomaly viewed from space. *Geophys. Res. Lett.* **41**, 6898–6903 (2014).
11. C. Frankenberg, A. K. Thorpe, D. R. Thompson, G. Hulley, E. A. Kort, N. Vance, J. Borchardt, T. Krings, K. Gerilowski, C. Sweeney, S. Conley, B. D. Bue, A. D. Aubrey, S. Hook, R. O. Green, Airborne methane remote measurements reveal heavy-tail flux distribution in Four Corners region. *Proc. Natl. Acad. Sci. U.S.A.* **113**, 9734–9739 (2016).
12. M. L. Smith, A. Gvakharia, E. A. Kort, C. Sweeney, S. A. Conley, I. Faloona, T. Newberger, R. Schnell, S. Schwietzke, S. Wolter, Airborne quantification of methane emissions over the four corners region. *Environ. Sci. Technol.* **51**, 5832–5837 (2017).
13. EIA, Drilling productivity report; https://www.eia.gov/petroleum/drilling/ [accessed 1 May 2019].
14. C. Krauss, "The 'monster' Texas oil field that made the U.S. a star in the world market," *New York Times*, 2019.
15. K. A. Willyard, G. W. Schade, Flaring in two Texas shale areas: Comparison of bottom-up with top-down volume estimates for 2012 to 2015. *Sci. Total Environ.* **691**, 243–251 (2019).
16. SRON, S5P Mission Performance Centre Methane [L2__CH4___] Readme, S5P-MPC-SRON-PRF-CH4, V01.03.02 (2019).

17. J. P. Veefkind, I. Aben, K. McMullan, H. Förster, J. de Vries, G. Otter, J. Claas, H. J. Eskes, J. F. de Haan, Q. Kleipool, M. van Weele, O. Hasekamp, R. Hoogeveen, J. Landgraf, R. Snel, P. Tol, P. Ingmann, R. Voors, B. Kruizinga, R. Vink, H. Visser, P. F. Levelt, TROPOMI on the ESA Sentinel-5 Precursor: A GMES mission for global observations of the atmospheric composition for climate, air quality and ozone layer applications. *Remote Sens. Environ.* **120**, 70–83 (2012).
18. EIA, The Wolfcamp play has been key to Permian Basin oil and natural gas production growth (2018); https://www.eia.gov/todayinenergy/detail.php?id=37532#tab1 [accessed 18 August 2019].
19. Y. Zhang, R. Gautam, D. Zavala-Araiza, D. J. Jacob, R. Zhang, L. Zhu, J.-X. Sheng, T. Scarpelli, Satellite-observed changes in Mexico's offshore gas flaring activity linked to oil/gas regulations. *Geophys. Res. Lett.* **46**, 1879–1888 (2019).
20. B. N. Duncan, L. N. Lamsal, A. M. Thompson, Y. Yoshida, Z. Lu, D. G. Streets, M. M. Hurwitz, K. E. Pickering, A space-based, high-resolution view of notable changes in urban NO_x pollution around the world (2005-2014). *J. Geophys. Res. Atmos.* **121**, 976–996 (2016).
21. J. X. Sheng, D. J. Jacob, A. J. Turner, J. D. Maasakkers, M. P. Sulprizio, A. A. Bloom, A. E. Andrews, D. Wunch, High-resolution inversion of methane emissions in the Southeast US using $SEAC^4RS$ aircraft observations of atmospheric methane: Anthropogenic and wetland sources. *Atmos. Chem. Phys.* **18**, 6483–6491 (2018).
22. EPA, Inventory of US greenhouse gas emissions and sinks: 1990–2017 (2019); https://www.epa.gov/ghgemissions/inventory-us-greenhouse-gas-emissions-and-sinks-1990-2017.
23. M. Buchwitz, O. Schneising, M. Reuter, J. Heymann, S. Krautwurst, H. Bovensmann, J. P. Burrows, H. Boesch, R. J. Parker, P. Somkuti, R. G. Detmers, O. P. Hasekamp, I. Aben, A. Butz, C. Frankenberg, A. J. Turner, Satellite-derived methane hotspot emission estimates using a fast data-driven method. *Atmos. Chem. Phys.* **17**, 5751–5774 (2017).
24. J. Peischl, S. J. Eilerman, J. A. Neuman, K. C. Aikin, J. de Gouw, J. B. Gilman, S. C. Herndon, R. Nadkarni, M. Trainer, C. Warneke, T. B. Ryerson, Quantifying methane and ethane emissions to the atmosphere from Central and Western U.S. oil and natural gas production regions. *J. Geophys. Res. Atmos.* **123**, 7725–7740 (2018).
25. X. Ren, D. L. Hall, T. Vinciguerra, S. E. Benish, P. R. Stratton, D. Ahn, J. R. Hansford, M. D. Cohen, S. Sahu, H. He, C. Grimes, J. D. Fuentes, P. B. Shepson, R. J. Salawitch, S. H. Ehrman, R. R. Dickerson, Methane emissions from the Marcellus Shale in Southwestern Pennsylvania and Northern West Virginia based on airborne measurements. *J. Geophys. Res. Atmos.* **124**, 1862–1878 (2019).
26. J. Peischl, T. B. Ryerson, K. C. Aikin, J. A. de Gouw, J. B. Gilman, J. S. Holloway, B. M. Lerner, R. Nadkarni, J. A. Neuman, J. B. Nowak, M. Trainer, C. Warneke, D. D. Parrish, Quantifying atmospheric methane emissions from the Haynesville, Fayetteville, and northeastern Marcellus shale gas production regions. *J. Geophys. Res. Atmos.* **120**, 2119–2139 (2015).
27. A. Karion, C. Sweeney, E. A. Kort, P. B. Shepson, A. Brewer, M. Cambaliza, S. A. Conley, K. Davis, A. Deng, M. Hardesty, S. C. Herndon, T. Lauvaux, T. Lavoie, D. Lyon, T. Newberger, G. Pétron, C. Rella, M. Smith, S. Wolter, T. I. Yacovitch, P. Tans, Aircraft-based estimate of total methane emissions from the Barnett Shale region. *Environ. Sci. Technol.* **49**, 8124–8131 (2015).
28. Z. R. Barkley, T. Lauvaux, K. J. Davis, A. Deng, N. L. Miles, S. J. Richardson, Y. Cao, C. Sweeney, A. Karion, M. K. Smith, E. A. Kort, S. Schwietzke, T. Murphy, G. Cervone, D. Martins, J. D. Maasakkers, Quantifying methane emissions from natural gas production in north-eastern Pennsylvania. *Atmos. Chem. Phys.* **17**, 13941–13966 (2017).
29. S. Schwietzke, G. Pétron, S. Conley, C. Pickering, I. Mielke-Maday, E. J. Dlugokencky, P. P. Tans, T. Vaughn, C. Bell, D. Zimmerle, S. Wolter, C. W. King, A. B. White, T. Coleman, L. Bianco, R. C. Schnell, Improved mechanistic understanding of natural gas methane emissions from spatially resolved aircraft measurements. *Environ. Sci. Technol.* **51**, 7286–7294 (2017).
30. J. Peischl, A. Karion, C. Sweeney, E. A. Kort, M. L. Smith, A. R. Brandt, T. Yeskoo, K. C. Aikin, S. A. Conley, A. Gvakharia, M. Trainer, S. Wolter, T. B. Ryerson, Quantifying atmospheric methane emissions from oil and natural gas production in the Bakken shale region of North Dakota. *J. Geophys. Res. Atmos.* **121**, 6101–6111 (2016).
31. A. Karion, C. Sweeney, G. Pétron, G. Frost, R. Michael Hardesty, J. Kofler, B. R. Miller, T. Newberger, S. Wolter, R. Banta, A. Brewer, E. Dlugokencky, P. Lang, S. A. Montzka, R. Schnell, P. Tans, M. Trainer, R. Zamora, S. Conley, Methane emissions estimate from airborne measurements over a western United States natural gas field. *Geophys. Res. Lett.* **40**, 4393–4397 (2013).
32. G. Pétron, A. Karion, C. Sweeney, B. R. Miller, S. A. Montzka, G. J. Frost, M. Trainer, P. Tans, A. Andrews, J. Kofler, D. Helmig, D. Guenther, E. Dlugokencky, P. Lang, T. Newberger, S. Wolter, B. Hall, P. Novelli, A. Brewer, S. Conley, M. Hardesty, R. Banta, A. White, D. Noone, D. Wolfe, R. Schnell, A new look at methane and nonmethane hydrocarbon emissions from oil and natural gas operations in the Colorado Denver-Julesburg Basin. *J. Geophys. Res. Atmos.* **119**, 6836–6852 (2014).
33. M. Omara, M. R. Sullivan, X. Li, R. Subramanian, A. L. Robinson, A. A. Presto, Methane emissions from conventional and unconventional natural gas production sites in the marcellus shale basin. *Environ. Sci. Technol.* **50**, 2099–2107 (2016).
34. RBN Energy, "Hell In Texas—Permian gas takeaway headed for capacity wall," RBN Energy Drill Down Report (2018).
35. EIA, Natural gas consumption by end use; https://www.eia.gov/dnav/ng/ng_cons_sum_dcu_STX_a.htm. [accessed 20 August 2019].
36. M. Etminan, G. Myhre, E. J. Highwood, K. P. Shine, Radiative forcing of carbon dioxide, methane, and nitrous oxide: A significant revision of the methane radiative forcing. *Geophys. Res. Lett.* **43**, 12,614–12,623 (2016).
37. T. Curtis, B. Montalbano, *The Permian Basin Produces Gas, Too—Permian Basin Oil and Gas Production Growth: A Case Study for Gas Infrastructure Needs in the U.S.* (Energy Policy Research Foundation Inc., 2018).
38. H. Hu, J. Landgraf, R. Detmers, T. Borsdorff, J. aan de Brugh, I. Aben, A. Butz, O. Hasekamp, Toward global mapping of methane with TROPOMI: First results and intersatellite comparison to GOSAT. *Geophys. Res. Lett.* **45**, 3682–3689 (2018).
39. H. Hu, O. Hasekamp, A. Butz, A. Galli, J. Landgraf, J. Aan de Brugh, T. Borsdorff, R. Scheepmaker, I. Aben, The operational methane retrieval algorithm for TROPOMI. *Atmos. Meas. Tech.* **9**, 5423–5440 (2016).
40. O. Hasekamp, A. Lorente, H. Hu, A. Butz, J. aan de Brugh, J. Landgraf, "Algorithm theoretical baseline document for Sentinel-5 Precursor methane retrieval (issue 1.10), SRON-S5P-LEV2-RP-001" (SRON, 2019).
41. J.-X. Sheng, D. J. Jacob, J. D. Maasakkers, Y. Zhang, M. P. Sulprizio, Comparative analysis of low-Earth orbit (TROPOMI) and geostationary (GeoCARB, GEO-CAPE) satellite instruments for constraining methane emissions on fine regional scales: Application to the Southeast US. *Atmos. Meas. Tech.* **11**, 6379–6388 (2018).
42. G. P. Brasseur, D. J. Jacob, *Modeling of Atmospheric Chemistry* (Cambridge Univ. Press, 2017).
43. C. L. Heald, D. J. Jacob, D. B. A. Jones, P. I. Palmer, J. A. Logan, D. G. Streets, G. W. Sachse, J. C. Gille, R. N. Hoffman, T. Nehrkorn, Comparative inverse analysis of satellite (MOPITT) and aircraft (TRACE-P) observations to estimate Asian sources of carbon monoxide. *J. Geophys. Res. Atmos.* **109**, D23306 (2004).
44. D. H. Cusworth, D. J. Jacob, J.-X. Sheng, J. Benmergui, A. J. Turner, J. Brandman, L. White, C. A. Randles, Detecting high-emitting methane sources in oil/gas fields using satellite observations. *Atmos. Chem. Phys.* **18**, 16885–16896 (2018).
45. M. M. Rienecker, M. J. Suarez, R. Todling, J. Bacmeister, L. Takacs, H.-C. Liu, W. Gu, M. Sienkiewicz, R. D. Koster, R. Gelaro, I. Stajner, J. E. Nielsen, "The GEOS-5 data assimilation system—Documentation of versions 5.0.1, 5.1.0, and 5.2.0" (NASA Tech. Rep. NASA/TM-2008-104606, NASA, 2008), vol. 27, 118 pp.; https://gmao.gsfc.nasa.gov/pubs/docs/Rienecker369.pdf.
46. E. J. Dlugokencky, A. M. Crotwell, P. M. Lang, J. W. Mund, M. E. Rhodes, Atmospheric methane dry air mole fractions from quasi-continuous measurements at Barrow, Alaska and Mauna Loa, Hawaii, 1986–2017, version: 2019-06-21; ftp://aftp.cmdl.noaa.gov/data/trace_gases/ch4/in-situ/surface/ (2018).
47. A. E. Andrews, J. D. Kofler, M. E. Trudeau, J. C. Williams, D. H. Neff, K. A. Masarie, D. Y. Chao, D. R. Kitzis, P. C. Novelli, C. L. Zhao, E. J. Dlugokencky, P. M. Lang, M. J. Crotwell, M. L. Fischer, M. J. Parker, J. T. Lee, D. D. Baumann, A. R. Desai, C. O. Stanier, S. F. J. De Wekker, D. E. Wolfe, J. W. Munger, P. P. Tans, CO_2, CO, and CH_4 measurements from tall towers in the NOAA Earth System Research Laboratory's Global Greenhouse Gas Reference Network: Instrumentation, uncertainty analysis, and recommendations for future high-accuracy greenhouse gas monitoring efforts. *Atmos. Meas. Tech.* **7**, 647–687 (2014).
48. C. Sweeney, A. Karion, S. Wolter, T. Newberger, D. Guenther, J. A. Higgs, A. E. Andrews, P. M. Lang, D. Neff, E. Dlugokencky, J. B. Miller, S. A. Montzka, B. R. Miller, K. A. Masarie, S. C. Biraud, P. C. Novelli, M. Crotwell, A. M. Crotwell, K. Thoning, P. P. Tans, Seasonal climatology of CO_2 across North America from aircraft measurements in the NOAA/ESRL Global Greenhouse Gas Reference Network. *J. Geophys. Res. Atmos.* **120**, 5155–5190 (2015).
49. J. D. Maasakkers, D. J. Jacob, M. P. Sulprizio, A. J. Turner, M. Weitz, T. Wirth, C. Hight, M. DeFigueiredo, M. Desai, R. Schmeltz, L. Hockstad, A. A. Bloom, K. W. Bowman, S. Jeong, M. L. Fischer, Gridded national inventory of U.S. methane emissions. *Environ. Sci. Technol.* **50**, 13123–13133 (2016).
50. Enverus DrillingInfo, DI Desktop (2019); didesktop.com.
51. EPA, Inventory of US greenhouse gas emissions and sinks: 1990–2014 (2016); https://www.epa.gov/ghgemissions/inventory-us-greenhouse-gas-emissions-and-sinks-1990-2014.
52. EDF, New Mexico oil & gas data (2019); https://www.edf.org/nm-oil-gas/ [accessed 18 August 2019].
53. A. J. Marchese, T. L. Vaughn, D. J. Zimmerle, D. M. Martinez, L. L. Williams, A. L. Robinson, A. L. Mitchell, R. Subramanian, D. S. Tkacik, J. R. Roscioli, S. C. Herndon, Methane emissions from United States natural gas gathering and processing. *Environ. Sci. Technol.* **49**, 10718–10727 (2015).
54. A. L. Mitchell, D. S. Tkacik, J. R. Roscioli, S. C. Herndon, T. I. Yacovitch, D. M. Martinez, T. L. Vaughn, L. L. Williams, M. R. Sullivan, C. Floerchinger, M. Omara, R. Subramanian, D. Zimmerle, A. J. Marchese, A. L. Robinson, Measurements of methane emissions

from natural gas gathering facilities and processing plants: Measurement results. *Environ. Sci. Technol.* **49**, 3219–3227 (2015).
55. C. Elvidge, M. Zhizhin, K. Baugh, F.-C. Hsu, T. Ghosh, Methods for global survey of natural gas flaring from visible infrared imaging radiometer suite data. *Energies* **9**, 14 (2016).
56. A. M. Robertson, R. Edie, D. Snare, J. Soltis, R. A. Field, M. D. Burkhart, C. S. Bell, D. Zimmerle, S. M. Murphy, Variation in methane emission rates from well pads in four oil and gas basins with contrasting production volumes and compositions. *Environ. Sci. Technol.* **51**, 8832–8840 (2017).
57. D. Zavala-Araiza, D. R. Lyon, R. A. Alvarez, K. J. Davis, R. Harriss, S. C. Herndon, A. Karion, E. A. Kort, B. K. Lamb, X. Lan, A. J. Marchese, S. W. Pacala, A. L. Robinson, P. B. Shepson, C. Sweeney, R. Talbot, A. Townsend-Small, T. I. Yacovitch, D. J. Zimmerle, S. P. Hamburg, Reconciling divergent estimates of oil and gas methane emissions. *Proc. Natl. Acad. Sci. U.S.A.* **112**, 15597–15602 (2015).

Acknowledgments: We thank the team that realized the TROPOMI instrument and its data products, consisting of the partnership between Airbus Defense and Space Netherlands, KNMI, SRON, and TNO, commissioned by NSO and ESA. Sentinel-5 Precursor is part of the EU Copernicus program, and Copernicus Sentinel data 2018–2019 have been used. We acknowledge the provision of publicly available VIIRS night-fire data. We also acknowledge NOAA Earth System Research Laboratory's Global Greenhouse Gas Reference Network for providing methane measurements at MLO, WKT, and TGC. **Funding:** This work was supported by the Kravis Scientific Research Fund, the Robertson Foundation, GALES project (#15597) by the Dutch Technology Foundation STW, and the TROPOMI national program through NSO. Y.Z. was funded by the Kravis Fellowship through EDF and by Harvard University. P.S. and S.P. are funded through the GALES project (#15597) by the Dutch Technology Foundation STW, which is part of the Netherlands Organization for Scientific Research (NWO). A.L. acknowledges funding from the TROPOMI national program through NSO. R.G., M.O., D.L., D.Z.-A., R.A.A., and S.P.H. were funded by the Robertson Foundation. D.J.J. was funded by the NASA Carbon Monitoring System. **Author contributions:** Y.Z. and R.G. led the study and wrote the manuscript with inputs from all coauthors; Y.Z. performed inversion simulations, carried out sensitivity experiments, and interpreted results with inputs from D.J.J.; S.P., P.S., S.H., A.L., and I.A. analyzed TROPOMI data and provided mass balance calculations; J.D.M. provided bottom-up inventory data analysis; M.O., D.L., D.Z.-A., R.A.A., and S.P.H. provided field measurement–based inventory data analysis; H.N. and M.P.S. contributed to setting up the nested GEOS-Chem simulation; D.J.V. evaluated GEOS-FP wind data; Y.Z. and R.Z. analyzed VIIRS radiant heat and TROPOMI NO_2 data; all authors provided scientific inputs during the analysis and reviewed and commented on the manuscript. **Competing interests:** The authors declare that they have no competing interests. **Data and materials availability:** All data needed to evaluate the conclusions in the paper are present in the paper and/or the Supplementary Materials. Spatially resolved methane emission estimates over the Permian Basin from this study (EI_{BU}, EI_{ME}, and the posterior estimate from atmospheric inverse modeling) can be accessed through https://doi.org/10.7910/DVN/NWQGHU. TROPOMI data are available through https://scihub.copernicus.eu/. VIIRS radiant heat data are available through https://eogdata.mines.edu/download_viirs_fire.html. The GEOS-Chem model is available at https://doi.org/10.5281/zenodo.1553349. Additional data related to this paper may be requested from the authors.

Submitted 16 September 2019
Accepted 19 March 2020
Published 22 April 2020
10.1126/sciadv.aaz5120

Citation: Y. Zhang, R. Gautam, S. Pandey, M. Omara, J. D. Maasakkers, P. Sadavarte, D. Lyon, H. Nesser, M. P. Sulprizio, D. J. Varon, R. Zhang, S. Houweling, D. Zavala-Araiza, R. A. Alvarez, A. Lorente, S. P. Hamburg, I. Aben, D. J. Jacob, Quantifying methane emissions from the largest oil-producing basin in the United States from space. *Sci. Adv.* **6**, eaaz5120 (2020).

ScienceAdvances

Quantifying methane emissions from the largest oil-producing basin in the United States from space

Yuzhong Zhang, Ritesh Gautam, Sudhanshu Pandey, Mark Omara, Joannes D. Maasakkers, Pankaj Sadavarte, David Lyon, Hannah Nesser, Melissa P. Sulprizio, Daniel J. Varon, Ruixiong Zhang, Sander Houweling, Daniel Zavala-Araiza, Ramon A. Alvarez, Alba Lorente, Steven P. Hamburg, Ilse Aben and Daniel J. Jacob

Sci Adv **6** (17), eaaz5120.
DOI: 10.1126/sciadv.aaz5120